

# JGR Solid Earth

## RESEARCH ARTICLE

10.1029/2021JB023325

### Key Points:

- One hundred two new and revised shear wave splitting measurements using teleseismic SKS, SKKS, and PKS phases are reported
- Predominantly Grid northeast-southwest oriented fast polarization directions are found across Antarctica
- Anisotropy can be attributed to relict lithospheric fabrics, plate motion-induced asthenospheric flow, and small-scale convection

### Supporting Information:

Supporting Information may be found in the online version of this article.

### Correspondence to:

E. M. Lucas,  
eml303@psu.edu

### Citation:

Lucas, E. M., Nyblade, A. A., Accardo, N. J., Lloyd, A. J., Wiens, D. A., Aster, R. C., et al. (2022). Shear wave splitting across Antarctica: Implications for upper mantle seismic anisotropy. *Journal of Geophysical Research: Solid Earth*, 127, e2021JB023325. <https://doi.org/10.1029/2021JB023325>

Received 28 SEP 2021

Accepted 9 MAR 2022

## Shear Wave Splitting Across Antarctica: Implications for Upper Mantle Seismic Anisotropy

Erica M. Lucas<sup>1</sup> , Andrew A. Nyblade<sup>1</sup> , Natalie J. Accardo<sup>1</sup> , Andrew J. Lloyd<sup>2</sup>, Douglas A. Wiens<sup>3</sup> , Richard C. Aster<sup>4</sup> , Terry J. Wilson<sup>5</sup>, Ian W. Dalziel<sup>6</sup> , Graham W. Stuart<sup>7</sup>, John Paul O'Donnell<sup>8</sup> , J. Paul Winberry<sup>9</sup> , and Audrey D. Huerta<sup>9</sup>

<sup>1</sup>Department of Geosciences, Pennsylvania State University, University Park, PA, USA, <sup>2</sup>Lamont-Doherty Earth Observatory, Columbia University, Palisades, NY, USA, <sup>3</sup>Department of Earth and Planetary Sciences, Washington University in St. Louis, St. Louis, MO, USA, <sup>4</sup>Department of Geosciences, Warner College of Natural Resources, Colorado State University, Fort Collins, CO, USA, <sup>5</sup>School of Earth Sciences, Ohio State University, Columbus, OH, USA, <sup>6</sup>Jackson School of Geosciences, University of Texas at Austin, Austin, TX, USA, <sup>7</sup>School of Earth and Environment, University of Leeds, Leeds, UK,

<sup>8</sup>Geological Survey of South Australia, Adelaide, SA, Australia, <sup>9</sup>Department of Geological Sciences, Central Washington University, Ellensburg, WA, USA

**Abstract** We examine upper mantle anisotropy across the Antarctic continent using 102 new shear wave splitting measurements obtained from teleseismic SKS, SKKS, and PKS phases combined with 107 previously published results. For the new measurements, an eigenvalue technique is used to estimate the fast polarization direction and delay time for each phase arrival, and high-quality measurements are stacked to determine the best-fit splitting parameters at each seismic station. The ensemble of splitting measurements shows largely NE-SW-oriented fast polarization directions across Antarctica, with a broadly clockwise rotation in polarization directions evident moving from west to east across the continent. Although the first-order pattern of NE-SW-oriented polarization directions is suggestive of a single plate-wide source of anisotropy, we argue the observed pattern of anisotropy more likely arises from regionally variable contributions of both lithospheric and sub-lithospheric mantle sources. Anisotropy observed in the interior of East Antarctica, a region underlain by thick lithosphere, can be attributed to relict fabrics associated with Precambrian tectonism. In contrast, anisotropy observed in coastal East Antarctica, the Transantarctic Mountains (TAM), and across much of West Antarctica likely reflects both lithospheric and sub-lithospheric mantle fabrics. While sub-lithospheric mantle fabrics are best associated with either plate motion-induced asthenospheric flow or small-scale convection, lithospheric mantle fabrics in coastal East Antarctica, the TAM, and West Antarctica generally reflect Jurassic—Cenozoic tectonic activity.

**Plain Language Summary** Seismic anisotropy, the directionally dependent variation in seismic wave speed, is widely considered to be one of the best indicators of past and present deformation and flow in the upper mantle. When the mantle deforms or flows, olivine crystals often become oriented in a systematic direction. Measurements of seismic anisotropy delineate the direction in which olivine crystals in the upper mantle are aligned and provide useful information about the tectonic history and current mantle flow in a region. In this study, we use seismic waves from distant earthquakes recorded at seismometers located in Antarctica to measure upper mantle anisotropy. Our measurements generally indicate that seismic waves travel the fastest in a northeasterly southwesterly direction in the upper mantle across much of Antarctica. The relatively uniform seismic anisotropy that we measure across Antarctica is suggestive of a single source of origin; however, we conclude that the observed anisotropy must arise from several sources, including past tectonic activity and active mantle flow beneath Antarctica.

## 1. Introduction

Measurements of seismic anisotropy yield valuable constraints on both past and present mantle deformation and flow, and shear wave splitting, a clear manifestation of anisotropy, has long been used to investigate the geometry and strength of upper mantle anisotropy (e.g., Long & Silver, 2009; Mainprice et al., 2000; Nicolas & Christensen, 1987; Savage, 1999; Silver, 1996). As the dominant mineral, olivine is generally thought to make the primary contribution to upper mantle anisotropy (e.g., Long & Silver, 2009). Thus, the geometry and magnitude of anisotropy depend on the symmetry, orientation, and strength of the crystallographic preferred

orientation of olivine, which, in turn, depends on the conditions of deformation (i.e., temperature, pressure, and stress; e.g., Karato et al., 2008; Mainprice et al., 2005). The manner in which olivine's principal axes align with respect to the shear direction is commonly categorized by crystallographic preferred orientation types, including A-type, B-type, C-type, D-type, and E-type (e.g., Karato et al., 2008). Previous studies in continental settings, including Antarctica (e.g., Accardo et al., 2014; Barklage et al., 2009; Graw & Hansen, 2017), have assumed that the commonly occurring A-type fabric (e.g., Bernard et al., 2019), which promotes the alignment of the olivine fast axis with the direction of maximum shear, provides the primary contribution to seismic anisotropy. This assumption has been recently corroborated for Marie Byrd Land (MBL) in West Antarctica by Chatzaras and Kruckenberg (2021), who determined that the A-type fabric is a primary contributor to upper mantle anisotropy by analyzing xenoliths from seven volcanic centers in western and central MBL.

In continental regions, shear wave splitting arising from the A-type deformational fabric in olivine often reflects anisotropic structure in both the lithospheric and sub-lithospheric mantle (see Fouch & Rondenay, 2006 for review). Because tectonic processes can produce a lattice preferred orientation (LPO) in olivine that may become “frozen into” the lithospheric mantle (i.e., fossil anisotropy), anisotropy in the lithospheric mantle is often associated with past tectonic activity. While fast shear wave polarization directions typically develop parallel to the extensional direction in rift settings (e.g., Savage, 1999; Silver & Chan, 1991), predominantly belt-parallel and/or sub-parallel fast polarization directions, suggestive of transpressive deformation in the lithospheric mantle, are found in many orogenic belts (e.g., Nicolas, 1993; Silver & Chan, 1991; Vauchez & Nicolas, 1991; White-Gaynor & Nyblade, 2017). Additionally, numerous seismic anisotropy studies have found that fast shear wave polarization directions are generally oriented parallel to the strike of shear zones, indicative of vertically coherent deformation of the crust and lithospheric mantle (e.g., Vauchez & Nicolas, 1991). Anisotropy in the sub-lithospheric mantle is often attributed to LPO in olivine imparted by asthenospheric flow, where fast polarization directions may result from absolute plate motion (APM), small-scale convection, plume flow, or other geodynamic processes (see Long & Silver, 2009 for review).

Here, we report 102 new and revised shear wave splitting measurements obtained from teleseismic SKS, SKKS, and PKS phases and characterize upper mantle azimuthal anisotropy across Antarctica using the new and revised measurements combined with 107 previously published measurements. The ensemble of measurements reveals consistent patterns of anisotropy, both spanning the continent and within individual tectonic terranes. We interpret these patterns of anisotropy in the context of the geologic history of Antarctica to gain insights into the sources of the anisotropy (i.e., lithospheric vs. sub-lithospheric mantle) and geodynamic processes acting on the Antarctic plate.

## 2. Tectonic Setting and Previous Geophysical Studies

The geologic configuration of Antarctica can be attributed to five major tectonic events (e.g., Boger, 2011; Torsvik et al., 2008), including: (a) the stabilization of Archean cratons into Paleoproterozoic crustal blocks, (b) the Mesoproterozoic Grenville orogeny associated with the formation of Rodinia, (c) the Neoproterozoic breakup of Rodinia, (d) the late-Proterozoic – Cambrian Ross/Pan-African orogen associated with the formation of Gondwana, and finally (e) the formation of the West Antarctic Rift System (WARS) concurrent with the Mesozoic breakup of Gondwana. The Transantarctic Mountains (TAM), a >3,000-km-long non-compressional mountain range (ten Brink et al., 1997) superimposed on a Neoproterozoic rifted margin (Dalziel, 1992; Goodge, 2020), divide West Antarctica (WANT) from East Antarctica (EANT; Figure 1).

EANT and WANT are physiographically, geologically, and geophysically distinct (e.g., Bayer et al., 2009; Boger, 2011; Dalziel, 1992; Golynsky et al., 2018; Lamarque et al., 2015; Lloyd et al., 2020; O'Donnell & Nyblade, 2014). EANT, a large Precambrian shield uncomfortably overlain by sedimentary units, is underlain by thick crust (~40–55 km; e.g., Brenn et al., 2017; Graw et al., 2016; Hansen et al., 2010; Lubes et al., 2018; O'Donnell & Nyblade, 2014; Pyle et al., 2010) and an upper mantle characterized by globally fast wave speeds (e.g., Lloyd et al., 2020). WANT, an assemblage of four discrete crustal blocks separated by subglacial basins, is characterized by a spatially variable crust (e.g., Baranov et al., 2021; Dunham et al., 2020) underlain by a heterogeneous upper mantle (e.g., Lloyd et al., 2020; Lucas et al., 2020, 2021; O'Donnell et al., 2019; Shen et al., 2018; White-Gaynor et al., 2019).

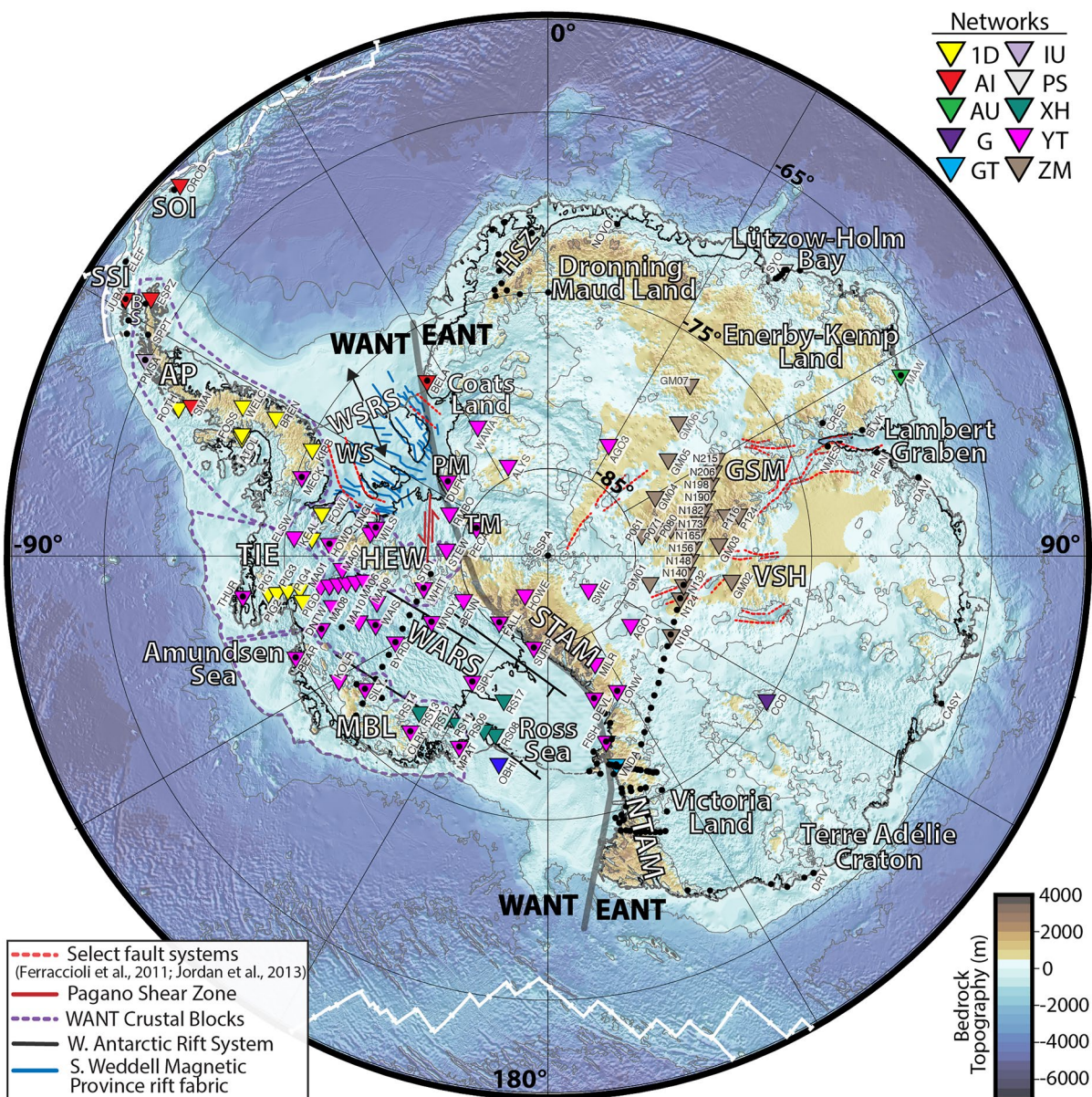


**Figure 1.** Seismic stations (triangles), colored by seismic network, used in this study plotted on a map of subglacial bedrock topography and bathymetry (Morlighem et al., 2020). Black circles mark the locations of previous shear wave splitting results. The nominal boundary between West Antarctica (WANT) and East Antarctica (EANT) is marked by a thick gray line. The grounding line and ice front position are delineated with black and gray points, respectively (Morlighem et al., 2020). Thin gray lines contour bedrock elevation from  $-6,000$  to  $4,500$  m in  $1,500$  m intervals. White lines mark plate boundaries (Bird, 2003). Abbreviated geographic features: AP: Antarctic Peninsula; BS: Bransfield Strait; GSM: Gamburtsev Subglacial Mountains; HEW: Haag-Ellsworth Whitmore crustal block; HSZ: Heimefront Shear Zone; MBL: Marie Byrd Land; NTAM: northern Transantarctic Mountains; PM: Pensacola Mountains; SOI: South Orkney Islands; SSI: South Shetland Islands; STAM: southern Transantarctic Mountains; TIE: Thurston Island-Eights Coast crustal block; TM: Thiel Mountains; VSH: Vostok Subglacial Highlands; WARS: West Antarctic Rift System; WS: Weddell Sea; WSRS: Weddell Sea Rift System.

Here, we note that because the discussion of geography near the South Pole can prove difficult, we employ the rectangular Grid coordinate system throughout this study. In the rectangular Grid coordinate system, north is oriented along the Prime Meridian and east is oriented along longitude  $90^{\circ}$ E.

## 2.1. East Antarctica

A mosaic of cratonic terranes compose the Precambrian shield of EANT (e.g., Boger et al., 2002; Boger, 2011; Ferraccioli et al., 2011; Harley et al., 2013; Tingey, 1991). Because of the expansive East Antarctic Ice Sheet,

the location, age, and nature of the cratons, mobile belts, and suture zones remain debated; however, the coastal terranes of EANT are well-correlated with conjugate terranes in Africa, India, Australia, and potentially Laurentia (e.g., Boger, 2011; Fitzsimons, 2000a, 2000b; Loewy et al., 2011). Related to the formation of the Nuna, Rodinia, and Gondwana supercontinents, the amalgamation of the EANT shield is attributed to Paleoproterozoic (~1.7–1.6 Ga), late Mesoproterozoic – Early Neoproterozoic (or Grenvillian, ~1.2–0.9 Ga), and Late Neoproterozoic – Early Paleozoic (or Pan-African, ~0.6–0.5 Ga) crustal assembly (e.g., Boger, 2011; Fitzsimons, 2000a, 2000b; Goodge & Fanning, 2016; Meert, 2003; Pierce et al., 2014). Our study area encompasses five main geographic regions of EANT, including (a) the Weddell Sea margin, (b) Dronning Maud Land (DML), (c) the Lambert Graben and Lützow-Holm Bay, (d) the Terre Adélie Craton (TAC), and (e) central EANT, including the Gamburtsev Subglacial Mountains (GSM) and Vostok Subglacial Highlands (VSH; Figure 1).

The Weddell Sea margin of EANT, as defined here, lies southeast of the Weddell Sea Rift System and encompasses the Pensacola and Thiel mountains (Figure 1). Development of the Pensacola and Thiel mountains has been attributed to deformation and batholith emplacement associated with the early Paleozoic Ross Orogeny (e.g., Ford, 1972; Goodge, 2020; Storey et al., 1996). Accardo et al. (2014) attributed regionally disparate fast shear wave polarization directions in the Pensacola and Thiel mountains to relict anisotropy predating the breakup of Gondwana (Figure 2).

Like much of East Antarctica, DML was impacted by numerous tectonic events, including mountain building during the Grenvillian orogeny, the assembly, and subsequent breakup of Gondwana (e.g., Boger, 2011; Fitzsimons, 2000a; Jacobs et al., 1998). With the exception of stations located in the Heimefront Shear Zone region, Müller (2001) and Bayer et al. (2007) find fast shear wave polarization directions oriented sub-parallel to the continental margin throughout DML (Figure 2). Bayer et al. (2007) reported NNE-SSW oriented fast polarization directions and generally higher magnitude delay times for stations located across the Heimefront shear zone (Figure 2).

East of the Lützow-Holm Bay region, the Lambert Rift extends from coastal EANT around the GSM and toward the South Pole region, constituting the East Antarctic rift system (e.g., Ferraccioli et al., 2011; Figure 1). With no indication of either current extension or large-scale Cenozoic rifting in EANT, the formation of the Lambert Rift and East Antarctic rift system has been attributed to a combination of Permian extension (~250 Ma) and Cretaceous strike-slip faulting associated with the breakup of Gondwana (~100 Ma; Phillips & Läufer, 2009). In contrast to the rest of EANT, both the Lützow-Holm Bay and Lambert Graben regions are underlain by slower mantle velocities and exhibit much greater variability in lithospheric thickness (e.g., Heeszel et al., 2013; Lloyd et al., 2020; Wiens et al., 2021). Reading and Heintz (2008) attribute margin-parallel fast polarization directions in the Lambert Graben region to relict structure resulting from the trans-tensional rifting of EANT and Australia at the breakup of Gondwana (Figure 2).

The TAC is a Neoarchean – Paleoproterozoic continental fragment that lacks much of the Neoproterozoic-Cambrian and Mesozoic tectonic reworking typical in other regions of EANT (Ménot et al., 2007; Figure 1). Potentially attributable to processes associated with the break-up of Gondwana, Lamarque et al. (2015) finds fast splitting directions oriented largely parallel to the continental margin and at a fairly high angle to regional crustal structures (Figure 2).

The mechanism responsible for the uplift of the GSM and VSH remains debated (e.g., An et al., 2015; Ferraccioli et al., 2011; Lloyd et al., 2013; Tabacco et al., 2006). Uplift of the GSM has been attributed to several mechanisms, including the Neoproterozoic-early Cambrian orogenic events associated with Gondwana assembly (e.g., Fitzsimons, 2003; Heeszel et al., 2013; Lloyd et al., 2013), Cretaceous rift-flank uplift (Ferraccioli et al., 2011), and far-field compression linked to the formation of Pangea (Veevers, 1994). Compared to other regions of EANT, the GSM and VSH are underlain by a thick lithosphere and fast upper mantle velocities (e.g., Hansen et al., 2010; Heeszel et al., 2013; Lloyd et al., 2013, 2020). Barklage et al. (2009) identified a slight clockwise rotation in fast polarization directions in the VSH compared to the fast polarization directions in the northern TAM (Figure 2).

## 2.2. West Antarctica

West Antarctica is comprised of four crustal blocks: MBL, the Antarctic Peninsula (AP), the Thurston Island-Eights Coast (TIE), and the Haag-Ellsworth-Whitmore Mountains (HEW; Figure 1). While the MBL, TIE, and

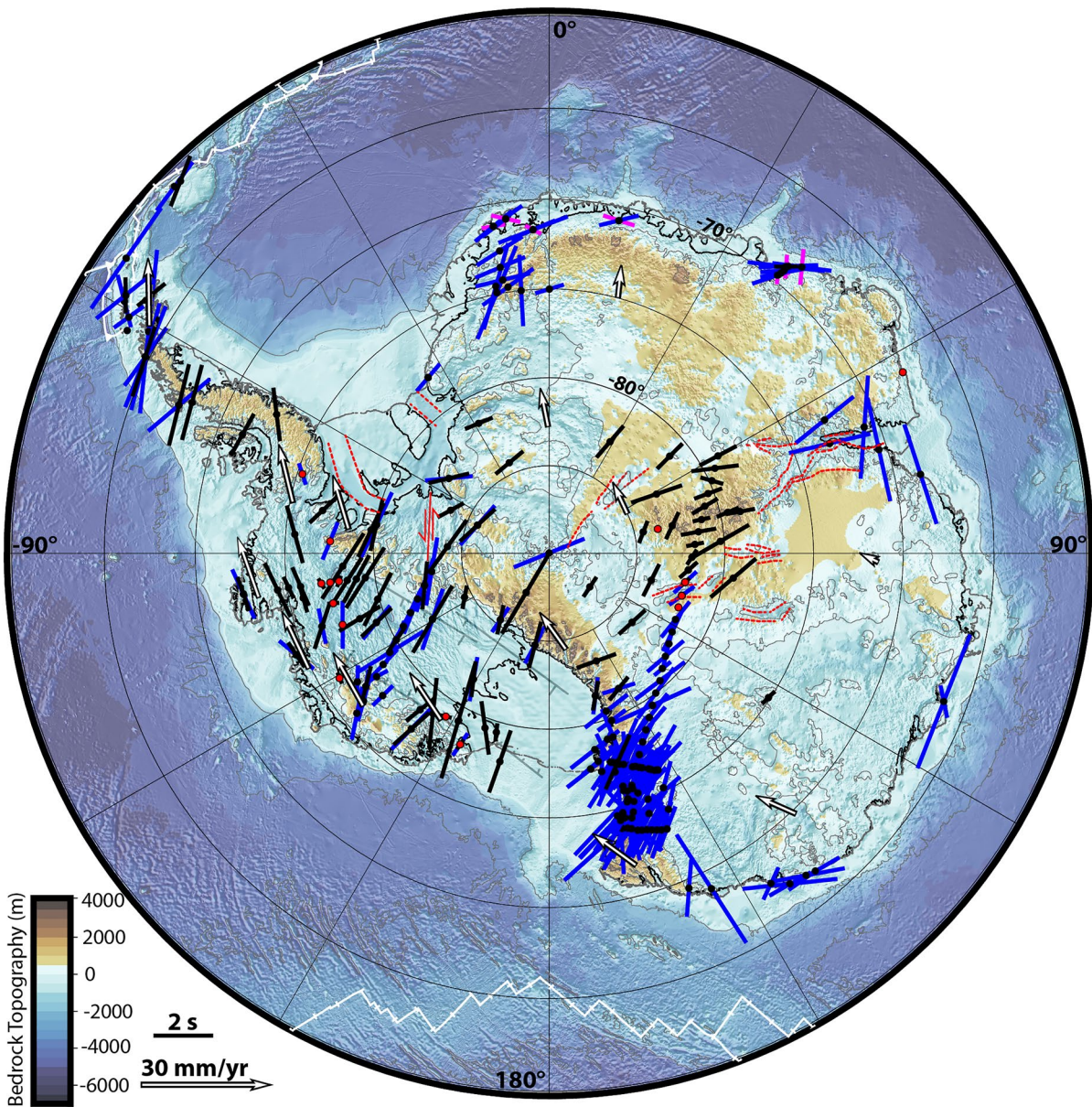


**Figure 2.** Stacked splitting results plotted on a map of subglacial bedrock topography and bathymetry (Morlighem et al., 2020). Bold black lines represent results from this study. Bold blue lines represent splitting results assembled from previous studies. Two-layer azimuthal anisotropy results, modeled by Müller (2001) and Usui et al. (2007) are plotted in blue (upper layer) and pink lines (lower layer). The orientation of the fast direction from the stacked solutions are shown with a blue or black line, and the length of the line is proportional to the splitting time (see scale in lower left of figure). Seismic stations with  $\delta t \geq 0.3$  s and  $\delta t < 0.3$  s are marked with black and red circles, respectively. White arrows plot the direction of Antarctic absolute plate motion in the hotspot reference frame calculated using HS3-NUVEL1A (Gripp & Gordon, 2002). Other geographic and tectonic features shown are the same as in Figure 1.

AP crustal blocks developed as fore-arc and magmatic-arc terranes along the paleo-Pacific convergent margin of Gondwana (e.g., Dalziel, 1992), the HEW is considered a fragment of the Transantarctic margin of EANT that underwent translation and rotation to its present position during the Jurassic opening of the Weddell Sea Rift System (e.g., Dalziel, 2007; Randall & Mac Niocaill, 2004; Schopf, 1969). HEW is separated from the three other blocks by the WARS (Dalziel & Elliot, 1982; Figure 1). The WARS is a region of thinned crust (e.g., Dunham et al., 2020; Shen et al., 2018) that underwent its major extensional phase during the Late Cretaceous (Siddoway, 2008). While largely underlain by an upper mantle characterized by wave speeds near the global average, numerous studies have imaged regional variability in upper mantle velocities within WANT (e.g., Lloyd et al., 2015; 2020; Lucas et al., 2020, 2021; O'Donnell et al., 2019; Shen et al., 2018; White-Gaynor et al., 2019).

Relatively fast velocity anomalies have been interpreted as lithosphere unmodified by tectonic activity since the Late Cretaceous formation of the WARS, and relatively slow velocity anomalies are suggestive of localized Cenozoic rifting (e.g., Lloyd et al., 2015, 2020; Lucas et al., 2020; O'Donnell et al., 2019; Shen et al., 2018). Accardo et al. (2014) reported fast polarization directions oriented subparallel to the inferred extension direction of the WARS and attributed the observed anisotropy to strain associated with a final pulse of Miocene extension in the western extent of the rift system (Figure 2). Recently, Zhou et al. (2022) attributed strong positive radial anisotropy (4%–8%) found throughout much of WANT's uppermost mantle to the preferred orientation of olivine due to tectonic activity.

MBL is defined by an uplifted dome centered on a belt of mid-to-late Cenozoic volcanoes (Figure 1). Many studies attribute Cenozoic magmatism in MBL to a mantle plume (e.g., Emry et al., 2015; Hansen et al., 2014; LeMasurier & Landis, 1996; Lloyd et al., 2020; Panter et al., 1997; Weaver et al., 1994), while others suggest subduction-related magma genesis (e.g., Finn et al., 2005). Consistent with the mantle plume hypothesis, numerous seismic studies have imaged deep low velocity anomalies beneath MBL (Emry et al., 2015; Hansen et al., 2014; Heeszel et al., 2016; Lloyd et al., 2015, 2020; Lucas et al., 2020; O'Donnell et al., 2019; Shen et al., 2018; Sieminski et al., 2003; White-Gaynor et al., 2019). However, rather than resembling a classic mantle plume anomaly, these low velocity anomalies form complex structures that span WANT and extend to great mantle depths (e.g., Phillips et al., 2018). Compared to elsewhere in WANT, Accardo et al. (2014) found weaker anisotropy in MBL (Figure 2) and noted that the anisotropic structure could reflect either mantle flow associated with a plume head or Cenozoic tectonic activity in the WARS.

Both the AP and TIE crustal blocks formed along the paleo-Pacific eastern margin of Gondwana, where the proto-Pacific plate was subducting throughout much of the Paleozoic and Mesozoic (e.g., Dalziel & Elliot, 1982; Storey et al., 1988). While subduction of the proto-Pacific plate beneath TIE and MBL ceased in the Mesozoic, the progressive shutdown of subduction from south to north along the AP margin has spanned from the Late Cretaceous to present-day (Barker, 1982; Larter & Barker, 1991). Likely related to the translation and rotation of the HEW, TIE rotated ~90° counterclockwise between 230 and 110 Ma (Grunow et al., 1991). Continental-scale and regional-scale tomography models show low velocities extending from MBL across the Amundsen Sea Embayment and TIE to the AP at upper mantle depths (Lloyd et al., 2020; Lucas et al., 2020; O'Donnell et al., 2019; Shen et al., 2018). While consistent fast polarization directions oriented sub-parallel to the coast have been found in TIE (Accardo et al., 2014), upper mantle anisotropy shows greater variability in the AP (Helffrich et al., 2002; Müller, 2001; Figure 2).

Compared to the other WANT crustal blocks, the HEW is underlain by thicker crust (30–40 km; e.g., Dunham et al., 2020) and regionally fast upper mantle velocities (e.g., Lloyd et al., 2020; Lucas et al., 2020). While the HEW was not internally deformed during the major extensional phase of the WARS during the Cretaceous, it underwent ~4 km of uplift during the Early Cretaceous (Fitzgerald & Stump, 1991). Sub-parallel to the direction of WARS extension, Accardo et al. (2014) found fast polarization directions in the HEW consistent with those measured throughout the adjacent WARS (Figure 2). Notably, when compared to broader WANT, Zhou et al. (2022) found the largest magnitudes of uppermost mantle radial anisotropy beneath the Whitmore Mountains.

### 2.3. Transantarctic Mountains

The TAM extend from northern Victoria Land to the Weddell Sea (Figure 1), and while the mechanisms responsible for uplift remain debated, the TAM are commonly interpreted as the uplifted flank of the WARS (e.g., Behrendt & Cooper, 1991; Brenn et al., 2017; Hansen et al., 2016; Stern & ten Brink, 1989; ten Brink et al., 1997). In addition to rift-flank uplift, TAM uplift has been attributed to the lateral conduction of heat from the WARS to EANT (Stern & ten Brink, 1989), thinning of the mantle lithosphere beneath the WARS, and crustal underplating associated with the WARS (Fitzgerald, 2002). After imaging slow uppermost mantle velocities extending across the TAM front and 350 km into EANT underlain by a relatively fast mantle root at ~200 km depth, Shen et al. (2018) attributed uplift in the southern TAM to the foundering of mantle lithosphere.

Along the TAM, both continental-scale and regional-scale tomographic studies reveal structural heterogeneity within the upper mantle that coincides with morphological changes of the mountain range (e.g., Brenn et al., 2017; Heeszel et al., 2016; Lloyd et al., 2020; O'Donnell et al., 2019; Shen et al., 2018; White-Gaynor et al., 2019). Previous studies have identified dominantly NE-SW fast polarization directions throughout the

TAM (e.g., Barklage et al., 2009; Graw & Hansen, 2017; Pondrelli et al., 2005; Salimbeni et al., 2010; Figure 2). In contrast to the predominantly NE-SW-oriented polarization directions, Pondrelli et al. (2005) and Salimbeni et al. (2010) measured Grid E-W to NNW-SSE oriented fast polarization directions at several seismic stations. While Salimbeni et al. (2010) suggests that the anisotropy measured mirrors tectonic structures associated with the Ross Orogeny, both the Barklage et al. (2009) and Graw and Hansen (2017) studies interpret anisotropic structure measured behind the TAM front and within the central TAM, respectively, as relict fabric predating the Ross Orogeny. Anisotropy observed along the Ross Sea coast has been attributed to both mantle flow associated with Cenozoic-aged extension and edge-driven convection associated with the sharp transition from thinner lithosphere in WANT to thicker lithosphere in EANT (Barklage et al., 2009; Graw & Hansen, 2017; Watson et al., 2006). Within central and West Antarctica, Zhou et al. (2022) finds the strongest positive radial anisotropy in the TAM uppermost mantle.

### 3. Data and Methods

#### 3.1. Data

From the analyses of data recorded on 102 semi-permanent and temporary broadband seismic stations operating between 1993 and 2021 (Figure 1 and Figure S1 and Table S1 in Supporting Information S1), we report new shear wave splitting measurements for 70 seismic stations and update splitting measurements for 32 stations included in previous studies (Accardo et al., 2014; Barklage et al., 2009; Hernandez et al., 2009; Kubo et al., 1995; Müller, 2001; Reading & Heintz, 2008; Usui et al., 2007; Figure 1; Table S3 in Supporting Information S1). When combined with 107 previously published splitting measurements (Accardo et al., 2014; Barklage et al., 2009; Bayer et al., 2007; Graw & Hansen, 2017; Helffrich et al., 2002; Hernandez et al., 2009; Lamarque et al., 2015; Müller, 2001; Pondrelli et al., 2005; Reading & Heintz, 2008; Salimbeni et al., 2010; Usui et al., 2007), our new and updated measurements can be used to characterize azimuthal anisotropy across much of Antarctica (Figures 1 and 2; Table S5 in Supporting Information S1).

#### 3.2. Methods

Shear wave splitting measurements were made in the MATLAB-based SplitLab software package (Wüstefeld et al., 2008) using waveforms from earthquakes with magnitudes ( $M_w$ )  $\geq 5.5$  and epicentral distances between  $90^\circ$  and  $140^\circ$ . SKS, SKKS, and PKS phases were identified and windowed in SplitLab, and only phases that were clearly separated from other phases were chosen for analysis. With the exception of seismograms with high signal-to-noise ratios (SNRs), most of the data were band-pass filtered with a low-frequency corner of 0.02 Hz and a variable high-frequency corner between 0.15 and 0.5 Hz. Splitting measurements in SplitLab were made using the method of Teanby et al. (2004). This method, which is based on the splitting correction method of Silver and Chan (1991), determines splitting parameters ( $\phi, \delta t$ ) via the minimization of particle motion energy on the transverse component. The Teanby et al. (2004) method is particularly advantageous as it checks for inconsistencies in splitting parameters over many measurement windows and thus removes subjectivity associated with manual window picking.

Results for each event-station pair were individually categorized as an A, B, or C quality based on several factors detailed in Table S2 in Supporting Information S1. Null measurements, rated as C quality measurements, do not exhibit energy on the transverse component of the rotated seismograms and can be attributed to an absence of anisotropy, an initial polarization of the incoming wave parallel or orthogonal to the fast anisotropic direction, or low SNR. The stacking method of Wolfe and Silver (1998), which produces a weighted sum of the individual misfit surfaces and provides a global solution for each station, was applied to A and B quality measurements to obtain robust stacked solutions. The number of individual measurements used in the final stacked solution for each seismic station is listed in Table S3 in Supporting Information S1, and the final stacked solutions for each station were categorized as A, B, or C quality results based on the back-azimuth sampling of the station and overall quality of the waveforms used in the stack (Table S2 in Supporting Information S1). We note that only the final stacked solutions and associated errors, obtained following the Wolfe and Silver (1998) stacking approach, are plotted in Figures 2–6 and Figure S4 in Supporting Information S1, and addressed in the following analysis and discussion.

While idealized single-layer uniform anisotropy models are often assumed initially, many studies invoke more complex anisotropy systems when splitting parameters vary as a function of back azimuth (e.g., Silver & Savage, 1994). For example, in the case of an anisotropic medium with two layers, apparent splitting parameters are expected to exhibit a characteristic  $\pi/2$  periodicity (Silver & Savage, 1994). In this study, we attempt to model two-layer anisotropic structure for stations with measurements showing a dependence between splitting parameter and back azimuth (Figure S3 in Supporting Information S1) but are unable to definitively assess the existence of two-layer anisotropy due to large azimuthal gaps in the data. Therefore, we interpret all splitting measurements made in this study using a single-layer model with uniform anisotropy.

#### 4. Results

Out of the 102 seismic stations used in this study, we determined stacked shear wave splitting parameters with a grade of B or better for 91 stations (Table S3 in Supporting Information S1). For 32 stations, we report updated results for stations included in previous studies (Accardo et al., 2014; Barklage et al., 2009; Hernandez et al., 2009; Kubo et al., 1995; Müller, 2001; Reading & Heintz, 2008; Salimbeni et al., 2010; Figures 1 and 2; Table S4 in Supporting Information S1). Our results, which include more individual splitting measurements compared to previous studies because of the increased time span of data availability, are generally consistent with previous splitting measurements (see Table S4 in Supporting Information S1). Eleven stations recorded either insufficient amounts of data or have poor quality data and are not used in the subsequent analyses and discussion (Table S3 in Supporting Information S1).

The shear wave splitting parameters, including the fast polarization direction ( $\phi$ ), splitting time ( $\delta t$ ), and associated errors (“ $\phi$  standard error” and “ $\delta t$  standard error”), are listed for each station in Table S3 in Supporting Information S1. When evaluated as a group, the 91 stations with a grade of B or better have a mean  $\phi$  standard error of  $5.4^\circ \pm 7.5^\circ$  (where the uncertainty is one-unit standard deviation), and a mean  $\delta t$  standard error of  $0.10 \pm 0.16$  s. The range of standard errors associated with our measurements is comparable to other studies utilizing similar approaches (e.g., Accardo et al., 2014; Barklage et al., 2009) and allows for a robust interpretation of anisotropy observed across Antarctica.

Out of the 91 seismic stations with a grade of B or better, 14 stations have  $\delta t$  of  $<0.3$  s (Figure 2; Table S3 in Supporting Information S1). Considering that the crust and ice layers combined may contribute up to  $\sim 0.3$  s to splitting times (e.g., Barklage et al., 2009) and  $\delta t > \sim 0.2$  s are typically associated with upper mantle anisotropy (e.g., Savage, 1999), seismic stations with  $\delta t < 0.3$  s likely correspond to either isotropic upper mantle fabric or vertical upper mantle flow. Stations with  $\delta t < 0.3$  s also generally show larger uncertainties in their respective  $\phi$  measurements (mean  $\phi$  standard error of  $13 \pm 10^\circ$ ) compared to stations with  $\delta t \geq 0.3$  s (mean  $\phi$  standard error of  $4 \pm 6^\circ$ ). Larger uncertainties of  $\phi$  for stations with  $\delta t < 0.3$  s are expected as the observed anisotropy may not predominantly reflect upper mantle anisotropy and, instead, may correspond to anisotropic contributions from the crust and/or ice. Therefore, we do not include  $\phi$  measurements corresponding to seismic stations with  $\delta t < 0.3$  s in Figure 3 nor consider them in the following analysis and discussion of splitting directions. However, we do include  $\delta t$  measurements of less than 0.3 s in the following analysis and discussion of delay times as they are likely indicative of regions with weak to no upper mantle anisotropy, which is important to constraining and investigating upper mantle anisotropy in continental regions. Again, note that we have converted  $\phi$  to the rectangular Grid coordinate system throughout the following analyses and discussion (see Table S3 in Supporting Information S1).

##### 4.1. East Antarctica

With  $\phi$  ranging from Grid  $21^\circ$  to  $106^\circ$  and  $\delta t$  from 0.1 to 1.3 s, splitting measurements exhibit notable variability across central EANT (Figure 3 and Figure S4 in Supporting Information S1). In central EANT, we find an average  $\phi$  and  $\delta t$  of  $53 \pm 19^\circ$  and  $0.6 \pm 0.3$  s, respectively (Figure 3 and Figure S4 in Supporting Information S1). An updated splitting measurement at seismic station SYO, in conjunction with measurements from Usui et al. (2007) and Reading and Heintz (2008), indicates that splitting measurements in the Lambert Graben – Lützow-Holm Bay region (LGLH) are generally oriented either N-S or E-W (Figures 1–3). Unlike Usui et al. (2007), we do not find convincing evidence of two-layer anisotropy at seismic station SYO in the Lützow-Holm Bay area (Figure S3h in Supporting Information S1).

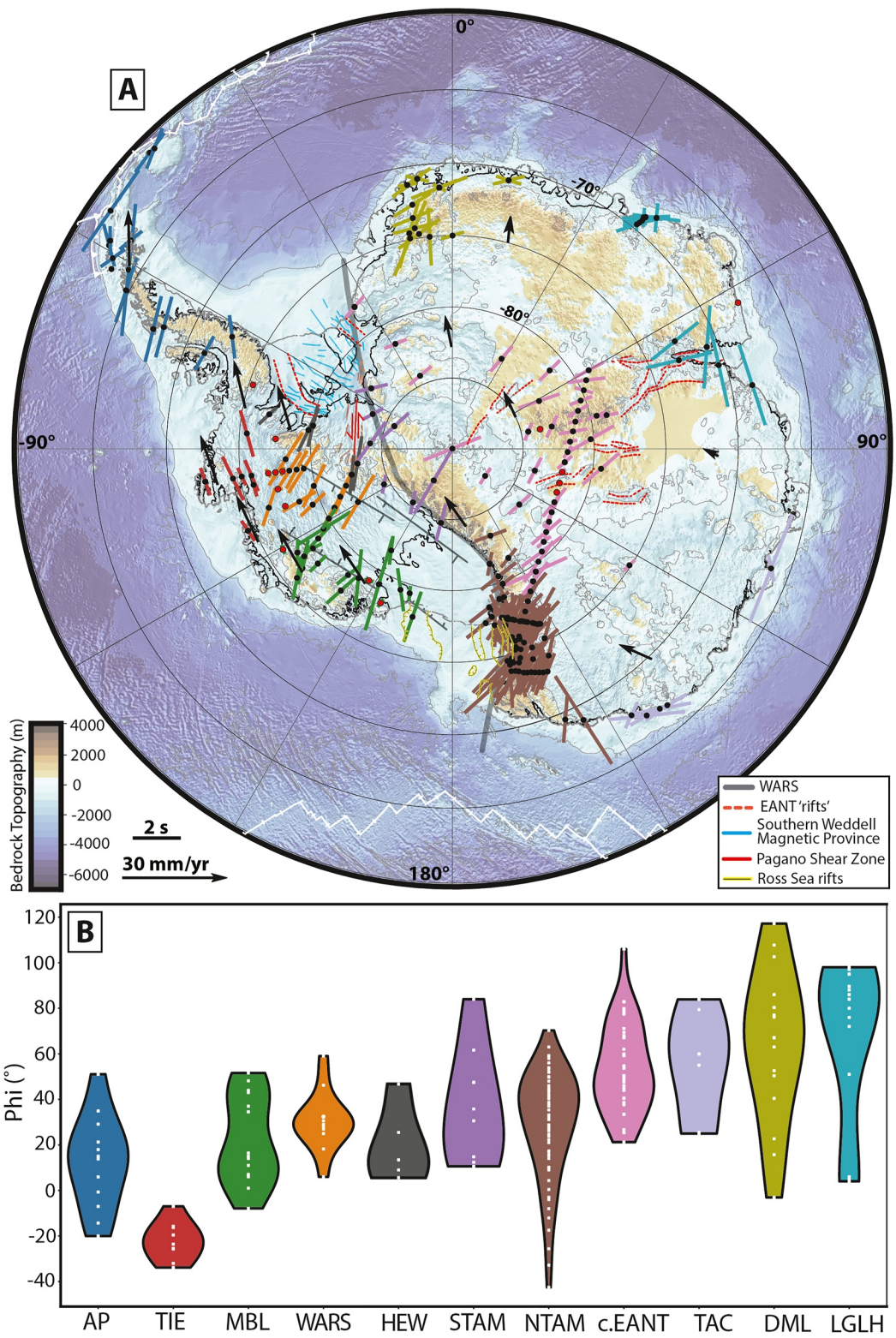


Figure 3.

#### 4.2. West Antarctica

Apart from seismic station ESPZ, the contiguous AP is characterized by NNE-SSW oriented  $\phi$  directions ( $-7^\circ$  to  $18^\circ$ ; Figures 1–3). The  $\phi$  measured at ESPZ is consistent with NE-SW-oriented  $\phi$  ( $21^\circ$ – $51^\circ$ ) measured at several stations located in the South Shetland Islands and South Orkney Islands (Figures 1–3). AP stations have a relatively large average  $\delta t$  of  $1.1 \pm 0.7$  s (Figure S4 in Supporting Information S1).

Of all the station groupings in Figure 3, seismic stations in the TIE crustal block show the greatest regional similarity in  $\phi$  (average  $\phi = -22.1 \pm 8.4^\circ$ ). Delay times in the TIE exhibit moderate variability, ranging from 0.4 to 1.0 s (average  $\delta t = 0.7 \pm 0.2$  s; Figure S4 in Supporting Information S1). Unlike the Accardo et al. (2014) study that found some variability in  $\phi$  directions across the TIE, we find notably uniform  $\phi$  directions (Figures 2 and 3).

Apart from seismic stations MA01, MA03, and MA08, we find relatively uniform  $\phi$  across the WARS (average  $\phi = 30 \pm 13^\circ$ , average  $\delta t = 1.0 \pm 0.2$  s; Figures 1–3 and Figure S4 in Supporting Information S1). We find low magnitude  $\delta t$  at MA01, MA03, and MA08 and, despite the low magnitude of  $\delta t$ , we measure  $\phi$  at MA01 and MA03 with relatively low standard error (Figures 1–3; Table S3 in Supporting Information S1). Discordant with  $\phi$  measured throughout the WARS,  $\phi$  at MA01 has a greater affinity with polarization directions in the TIE crustal block (Figures 1–3). Likely because more individual splitting measurements are incorporated into the final stacked solutions in this study, the splitting parameters that we measure at DNTW and WNDY differ notably from those found in the Accardo et al. (2014) study (Figures 1 and 2; Table S4 in Supporting Information S1).

Polarization directions measured at seismic stations located in the HEW range from  $6^\circ$  to  $47^\circ$ , with an average of  $20 \pm 17^\circ$  (Figure 3). The greatest departure from the average  $\phi$  is found at FOWL (Figures 1–3). Not accounting for the low magnitude  $\delta t$  measured at HOWD (0.1 s), we find an average splitting magnitude of  $\delta t = 1.0 \pm 0.2$  s in the HEW (Figure S4 in Supporting Information S1).

After updating stations with previously reported splitting parameters and adding new measurements from numerous stations located adjacent to the Ross Sea, we find relatively consistent  $\phi$  and spatially variable  $\delta t$  across MBL (Figures 1–3 and Figure S4 in Supporting Information S1). We measure  $\phi$  and  $\delta t$  range from  $-8^\circ$  to  $52^\circ$  and 0.2–2.0 s, respectively, spanning MBL (Figure 3 and Figure S4 in Supporting Information S1).

#### 4.3. Transantarctic Mountains

Based on station location, we divide the TAM splitting measurements into two groups (northern TAM and southern TAM; Figure 3 and Figure S4 in Supporting Information S1). Both the northern TAM (NTAM) and southern TAM (STAM) groups show significant variability in  $\phi$  and  $\delta t$  (Figure 3 and Figure S4 in Supporting Information S1). Like previous studies (Barklage et al., 2009; Graw & Hansen, 2017; Pondrelli et al., 2005; Salimbeni et al., 2010), we find  $\phi$  ranging from  $-43^\circ$  to  $70^\circ$  (average  $\phi = 29 \pm 24^\circ$ ) and  $\delta t$  between 0.1 and 2.6 s (average  $\delta t = 1.2 \pm 0.5$  s) in the NTAM group (Figure 3 and Figure S4 in Supporting Information S1). Polarization directions in the STAM range from  $11^\circ$  to  $84^\circ$  (average  $\phi = 37 \pm 26^\circ$ ; Figure 3) and the measurements have an average  $\delta t = 0.8 \pm 0.4$  s (Figure S4 in Supporting Information S1).

### 5. Discussion

Shear wave splitting measurements indicate that upper mantle anisotropy across Antarctica is largely characterized by NE-SW-oriented  $\phi$  directions, with a clockwise rotation in  $\phi$  broadly evident from west to east across the continent (Figure 3). This first-order pattern in  $\phi$  raises the question: does the pattern of NE-SW-oriented  $\phi$  reflect a single source of anisotropy within the upper mantle and, if not, can sources of anisotropy in the lithospheric and sub-lithospheric mantle compound to produce the observed pattern in  $\phi$  directions? We address that question in this section. However, because we are unable to constrain multiple layers of anisotropy with our data and much

**Figure 3.** (a) Splitting results shown in Figure 2 color-coded by geographic region. Seismic stations with  $\delta t \geq 0.3$  s and  $\delta t \leq -0.3$  s are marked with black and red circles, respectively. Black arrows plot the direction of Antarctic absolute plate motion in the hotspot reference frame calculated using HS3-NUVEL1A (Gripp & Gordon, 2002). (b) Violin plot of  $\phi$  where color corresponds to the color of splitting results in (a). Individual splitting measurements are plotted as white points within each violin. The violin plot, in which the curves of each violin correspond to the density of  $\phi$  measurements, can be used to compare the distribution of splitting measurements in different regions of Antarctica. Abbreviated geographic features: DML: Dronning Maud Land; (c)EANT: central East Antarctica; LGLH: Lambert Graben – Lützow-Holm Bay region; TAC: Terre Adélie Craton. Other geographic features have the same abbreviations as in Figure 1. Tectonic features shown are also the same as in Figure 1.

of Antarctica's geology is obscured by ice cover, we acknowledge that different sources of anisotropy could be present locally or regionally and arguing definitively for a particular source of anisotropy is challenging.

### 5.1. Anisotropy From a Single Source

The first-order pattern of NE-SW-oriented  $\phi$  could arise from several standalone sources, such as fossil anisotropy, plate-scale mantle flow, or smaller-scale flow regimes in the mantle (e.g., Fouch & Rondenay, 2006). However, with the complex tectonic history of Antarctica, it seems highly unlikely that the observed anisotropy pattern results from fossil anisotropy alone. For this to be the case, collisional boundaries and extension directions would have to systematically align and, to be consistent with the splitting measurements, rotate clockwise across the continent. There is little geological evidence for this (e.g., Boger, 2011; Fitzsimons, 2000a, 2000b; Golynsky et al., 2018; Jordan et al., 2020; Siddoway, 2008).

The motion of a plate over the mantle can also induce asthenospheric shear strain and produce seismic anisotropy. In this case, the axis of shear is expected to align with the direction of plate motion relative to the ambient mantle and produce  $\phi$  oriented parallel to APM (Wang et al., 2008). However, as much of the observed  $\phi$  directions are not oriented parallel to APM directions (Gripp & Gordon, 2002; Figures 2 and 3), it is unlikely that upper mantle anisotropy arises solely from shear associated with the motion of the Antarctic lithosphere over the mantle. We also plot the ensemble of splitting measurements on the Faccenna et al. (2008) model of mantle tractions specific to Antarctica resulting from plate motion and density-driven flow (Figure 4) and find several isolated regions where  $\phi$  directions are well-aligned with sub-lithospheric tractions. Overall, however, there is considerable mismatch between  $\phi$  directions and sub-lithospheric tractions across Antarctica in the Faccenna et al. (2008) model. Thus, the observed NE-SW-oriented  $\phi$  pattern cannot be readily attributed solely to asthenospheric shear strain associated with either APM or density-driven flow.

Several smaller-scale (i.e., regional) mantle flow regimes have been inferred from seismic imaging in Antarctica, including flow associated with the MBL mantle plume (e.g., Lloyd et al., 2020; Lucas et al., 2020; O'Donnell et al., 2019), active subduction in the AP (e.g., Lloyd et al., 2020), and edge-driven convection in the TAM (Shen et al., 2018). When combined, these mantle flow regimes would not give rise to a NE-SW-oriented  $\phi$  pattern in WANT, and smaller-scale mantle flow beneath EANT has not been proposed previously. Therefore, the continent-scale clockwise rotation of fast polarization directions observed across Antarctica is also unlikely to be a reflection of regional variations in smaller-scale mantle flow.

### 5.2. Anisotropy From Several Sources

Having ruled out a single plate-wide source for the largely NE-SW-oriented  $\phi$  pattern (Figure 3), it follows that the observed  $\phi$  directions more likely arise from either a single source within a particular region or, alternatively, two or more sources (i.e., fossil anisotropy, plate motion-induced asthenospheric flow, and small-scale convection). To examine which sources may contribute to the observations on a region-by-region basis, a few additional observations need to be considered. (a) It is widely accepted that the dislocation creep regime needed to produce LPO in olivine extends to depths of  $\sim$ 200–400 km (e.g., Karato & Wu, 1993; Mainprice et al., 2005; Podolefsky et al., 2004). Given the large variability in lithospheric thickness in Antarctica (Figure 5a), it is possible that splitting observations in some regions could arise only from fossil anisotropy in the lithosphere, whereas in other areas with thinner lithosphere, anisotropy in the asthenosphere likely contributes to the observed splitting as well. In other words, the lithospheric mantle may not be sufficiently thick to cause the observed splitting times in some locations. (b) We generally find somewhat weaker anisotropy (average  $\delta t = 0.6 \pm 0.3$  s) at stations underlain by thick lithosphere ( $\geq 170$  km) and faster sub-lithospheric mantle compared to thinner lithosphere ( $< 170$  km) and slower sub-lithospheric mantle (average  $\delta t = 1.0 \pm 0.5$  s; Figures 5 and 6). However, there is considerable variability in  $\delta t$  within regions of both thicker and thinner lithosphere (Figure S5 in Supporting Information S1); therefore, it is prudent not to place undue importance on the small difference in  $\delta t$  of 0.4 s. Nevertheless, this observation is consistent with the Zhou et al. (2022) model of radial anisotropy in west and central Antarctica, which shows stronger radial anisotropy on average in the uppermost mantle beneath WANT and TAM compared to the interior of EANT. Therefore, the spatial patterns of both azimuthal and radial anisotropy observed in Antarctica may suggest that regions with recent tectonic activity and thinner lithosphere have stronger contributions from sub-lithospheric mantle anisotropy compared to regions characterized by prolonged tectonic quiescence.

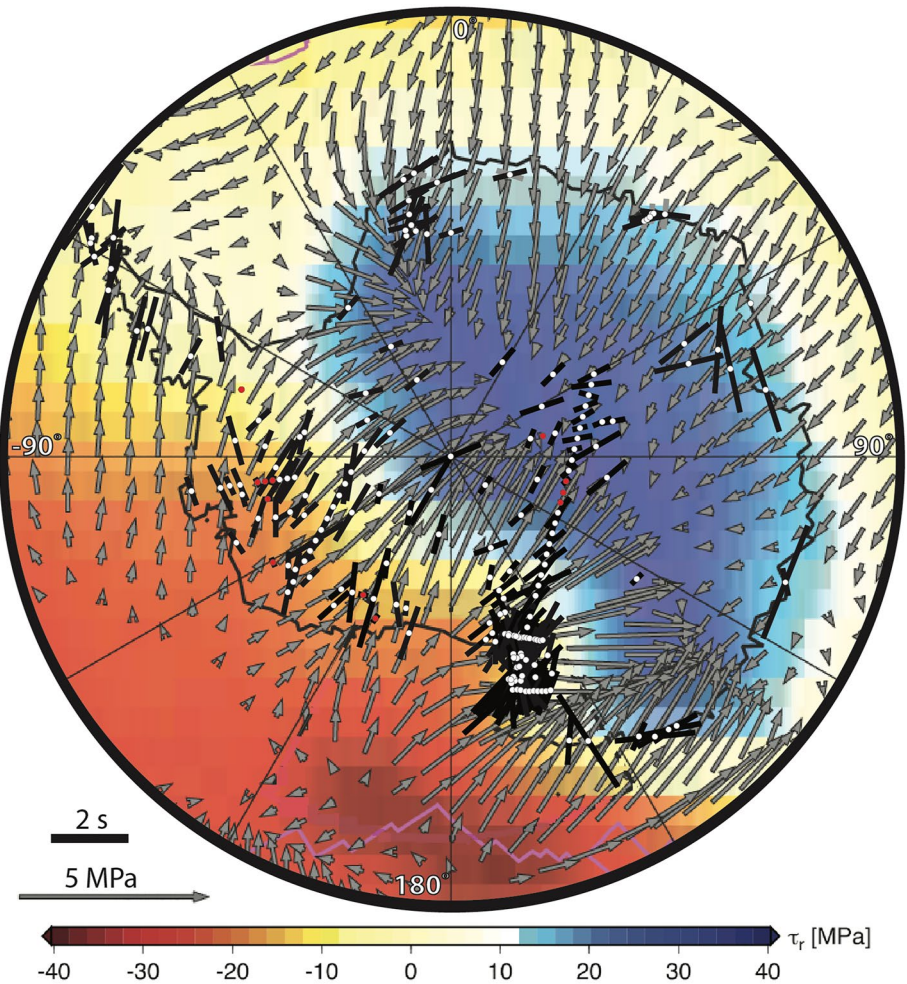


**Figure 4.** Splitting results shown in Figure 3 (black lines) plotted on the Faccenna et al. (2008) model of mantle tractions exerted by mantle drag on the lithosphere at 100 km depth. Faccenna et al. (2008) estimate mantle flow beneath Antarctica by a large-scale flow computation that incorporates the effect of plate motions and mantle density anomalies based on the SMEAN tomography model (Becker & Boschi, 2002; Becker & O'Connell, 2001). Red and blue colors correspond with negative (uplift) and positive (depression) radial forces, respectively, in the Faccenna et al. (2008) model. Seismic stations with  $\delta t \geq 0.3$  s and  $\delta t < 0.3$  s are marked with white and red circles, respectively.

### 5.2.1. East Antarctica

#### 5.2.1.1. Central East Antarctica (Figure 3)

Largely underlain by a thick ( $\geq 170$  km) lithosphere (Figure 5a), anisotropy observed across much of central EANT can be attributed solely to relict lithospheric fabrics (i.e., fossil anisotropy). Because NE-SW-oriented  $\phi$  found in central EANT are not likely wholly attributable to the NE-SW direction of shortening characteristic of the Ross Orogeny, the last major tectonic event to directly impact EANT (e.g., Allibone, 1987; Findlay et al., 1984; Stump, 1995), anisotropy observed in central EANT more likely reflects relict fabrics associated with Precambrian tectonism (e.g., Boger, 2011; Torsvik et al., 2008). Several processes associated with the Precambrian amalgamation of proto-Antarctica could have contributed to the observed anisotropy, including the Neoproterozoic rifting of the Mawson Craton from Laurentia, widespread Late Paleoproterozoic – Early Mesoproterozoic magmatism, and/or the Late Mesoproterozoic rifting of the Darling Fault (e.g., Boger, 2011).

Central EANT encompasses both the GSM and VSH (Figures 1 and 3), and, while we note that Ferraccioli et al. (2011) attributed the uplift of the GSM and VSH to Permian-Cretaceous extension and transtension in EANT, we cannot reasonably attribute the anisotropic fabric found in the GSM and VSH to Phanerozoic tectonism because of the presence of a thick, cold lithosphere (e.g., Lloyd et al., 2013, 2020). As described by Lloyd

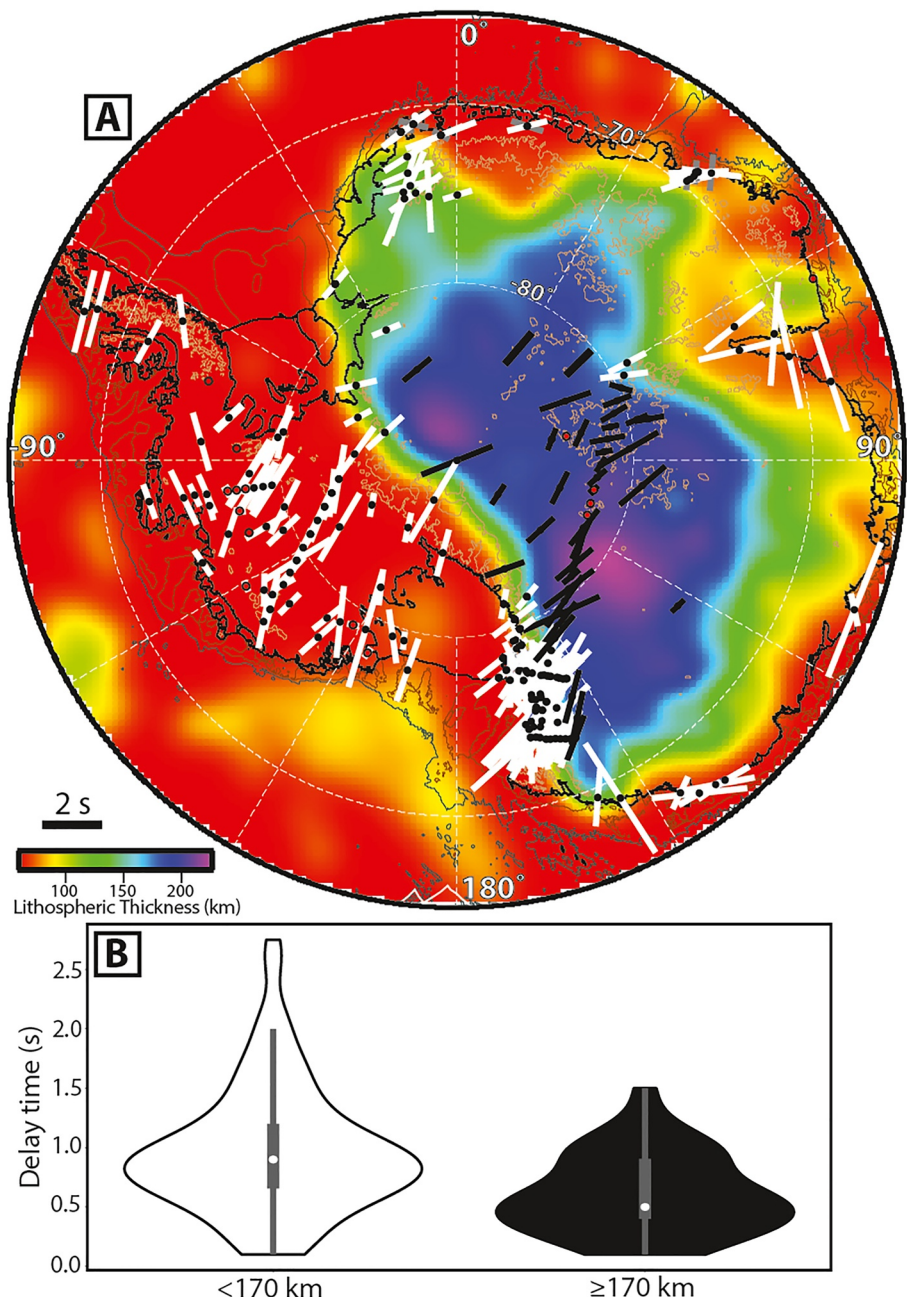


**Figure 5.** (a) Splitting results plotted on a map of Antarctic lithospheric thickness (Wiens et al., 2021). Seismic stations with  $\delta t \geq 0.3$  s and  $\delta t < 0.3$  s are marked with black and red circles, respectively. Splitting results are color-coded by lithospheric thickness, where white and black lines represent splitting measurements from stations underlain by  $<170$  km and  $\geq170$  km thick lithosphere, respectively. (b) Violin plot of delay times, where color corresponds to the color of splitting results in (a). Box plots, showing the median (white circle), quartiles (thick gray line), and distribution (thin gray line) of the respective delay time data set, are plotted within each violin.

et al. (2013), if the EANT craton had undergone Permian-Cretaceous extension and transtension, a thermal anomaly associated with lithospheric thinning would persist to the present and be evident in the seismological models as a low velocity anomaly. Instead, like the rest of central EANT, anisotropy in the GSM and VSH is best attributed to fossil anisotropy from Precambrian tectonism.

Additionally, although seismic stations BELA, WAWA, and DRV fall within the central EANT subdivision in Figure 3, all three stations are underlain by relatively slow upper mantle velocities and thinner lithosphere

compared to greater central EANT (Figures 1, 5, and 6). With thinner lithosphere and slower upper mantle seismic velocities, anisotropy observed at these stations likely reflects more recent tectonism, such as the Jurassic extension of the Weddell Sea Rift System (e.g., Jordan et al., 2017) or other processes associated with the breakup of Gondwana.

#### 5.2.1.2. Dronning Maud Land (Figure 3)

Müller (2001) and Bayer et al. (2007) argue that NE-SW and ENE-WSW oriented  $\phi$  directions found in DML reflect relict fabrics associated with Precambrian tectonism and the rifting of Gondwana, respectively (Figures 2 and 3). Both studies dismiss any contribution of active asthenospheric flow to the observed anisotropy; however, because much of DML has <150 km thick lithosphere (Figure 5a), the observed anisotropy likely reflects, at least in part, active asthenospheric flow, as suggested by Reading and Heintz (2008). Of the stations located in DML, anisotropy measurements at near-coastal stations most likely reflect asthenospheric fabrics as they are underlain by even thinner lithosphere (<75 km) and relatively slow upper mantle velocities (e.g., Lloyd et al., 2020; Figures 5 and 6). Polarization directions found in coastal DML stations are oriented nearly parallel to the continental margin (Figure 3), consistent with an asthenospheric fabric resulting from an edge-driven convection flow regime (e.g., King & Anderson, 1998).

#### 5.2.1.3. Lambert Graben – Lützow-Holm Bay Region (Figure 3)

Splitting measurements in the Lambert Graben region can be separated into two groups – one including seismic stations with fast polarization directions oriented parallel to the general trend of the EANT coastal margin and a second group comprised of stations with  $\phi$  directions oriented approximately normal to the continental margin (Figure 3). Reading and Heintz (2008) argued that both margin-normal and margin-parallel oriented  $\phi$  directions can be attributed to relict lithospheric fabrics; however, in a region characterized by relatively large magnitude splitting times (average  $\delta t = 1.6 \text{ s} \pm 0.2 \text{ s}$ ) and thin lithosphere (<100 km; Figure 5a), asthenospheric fabrics likely contribute, at least in part, to the observed anisotropy. Similar to DML, margin-parallel  $\phi$  directions may reflect an edge-driven convection flow regime. In contrast, margin-normal  $\phi$  directions, which trend sub-parallel to mantle tractions modeled by Faccenna et al. (2008) (Figure 4), may reflect APM-induced asthenospheric flow in addition to relict fabrics.

Using a two-layer anisotropy model, Usui et al. (2007) found predominantly N-S and E-W oriented  $\phi$  directions in the Lützow-Holm Bay region. Usui et al. (2007) attributed N-S oriented  $\phi$  directions to an upper layer of anisotropy reflecting processes associated with the amalgamation and subsequent break-up of Gondwana and E-W oriented  $\phi$  directions to APM-induced asthenospheric flow. However, considering the misalignment between  $\phi$  directions and APM-induced sub-lithospheric tractions (Figure 4), smaller-scale convective processes, such as edge-driven convection, are more likely to have an influence on the lower layer of anisotropy than APM-induced flow.

### 5.2.2. West Antarctica and Transantarctic Mountains

Interpreting upper mantle anisotropy in WANT and the TAM is difficult because the Transantarctic margin of EANT has been affected by seven tectonic events spanning ~750 million years that all could have contributed to the largely Grid NE-SW-oriented  $\phi$  directions found across the region (Figure 3). These seven tectonic events, which likely induced large-scale shear in near-parallelism, include: (a) Neoproterozoic rifting at the Transantarctic margin of the EANT craton (~750 Ma), (b) Ross-Delamerian subduction and orogeny (~530–500 Ma), (c) Late Paleozoic-Cenozoic subduction along the paleo-Pacific margin of Gondwana, (d) latest Paleozoic – earliest Mesozoic Gondwanide folding in HEW and Pensacola Mountains, (e) Jurassic-Cretaceous rifting initiating the breakup of Gondwana, (f) Late Cretaceous breakup of Zealandia from MBL, and (g) localized Cenozoic rifting in the WARS (e.g., Boger, 2011; Dalziel & Elliot, 1982; Jordan et al., 2020; Siddoway, 2008). In addition to assessing potential contributions from plate motion-induced asthenospheric flow and secondary convection, we evaluate potential contributions from the seven aforementioned tectonic events to upper mantle anisotropy observed on a regional basis (i.e., crustal blocks in WANT, northern TAM, and southern TAM) in the following sections.

#### 5.2.2.1. West Antarctic Rift System (Figure 3)

Similar to Accardo et al. (2014), we find extension-parallel  $\phi$  directions across the WARS (Figure 3). While Accardo et al. (2014) suggest that extension-parallel  $\phi$  reflects Cenozoic extension in the WARS,  $\phi$  directions are

perhaps best attributed to the major Cretaceous – early Cenozoic extensional phase (e.g., Siddoway, 2008). Indicative of tectonic quiescence, recent seismic imaging finds near-average upper mantle velocities beneath much of the WARS (Lloyd et al., 2020; Figure 6); therefore, uniform  $\phi$  measurements found across the WARS most likely reflect an anisotropic fabric that developed during the Cretaceous and was retained in the upper mantle. Although the major phase of extension occurred during the late Cretaceous – early Cenozoic, there is evidence for localized Cenozoic rifting in the WARS (e.g., Golynsky et al., 2018; Granot et al., 2010, 2013; Jordan et al., 2010; Lloyd et al., 2015; Lucas et al., 2020; O'Donnell et al., 2019); therefore, local variability in splitting measurements observed at a number of stations across the WARS (DNTW, MA10, UPTW, WAIS) may reflect fabrics associated with Cenozoic extension (Figures 1–3). Because the WARS is underlain by a relatively thin lithosphere (<80 km; Figure 5a), the observed anisotropy likely reflects sub-lithospheric fabrics in addition to lithospheric fabrics associated with the extension of the rift system. Suggestive of a contribution from APM-induced asthenospheric flow,  $\phi$  directions trend parallel/sub-parallel to both APM directions (Gripp & Gordon, 2002, Figure 3) and mantle tractions throughout much of the WARS (Figure 4).

#### 5.2.2.2. Haag Nunataks – Ellsworth Whitmore Mountains Crustal Block (Figure 3)

Given the relative similarity of polarization directions found in the HEW (average  $\phi = 20 \pm 17^\circ$ ) with polarization directions in the WARS (average  $\phi = 30 \pm 13^\circ$ ), HEW anisotropy may be attributable to the Late Cretaceous extension of the WARS (Figure 3). In this case, as suggested by Accardo et al. (2014), the same anisotropic fabric produced during the extension of the WARS would extend east beneath the HEW. Alternatively, HEW

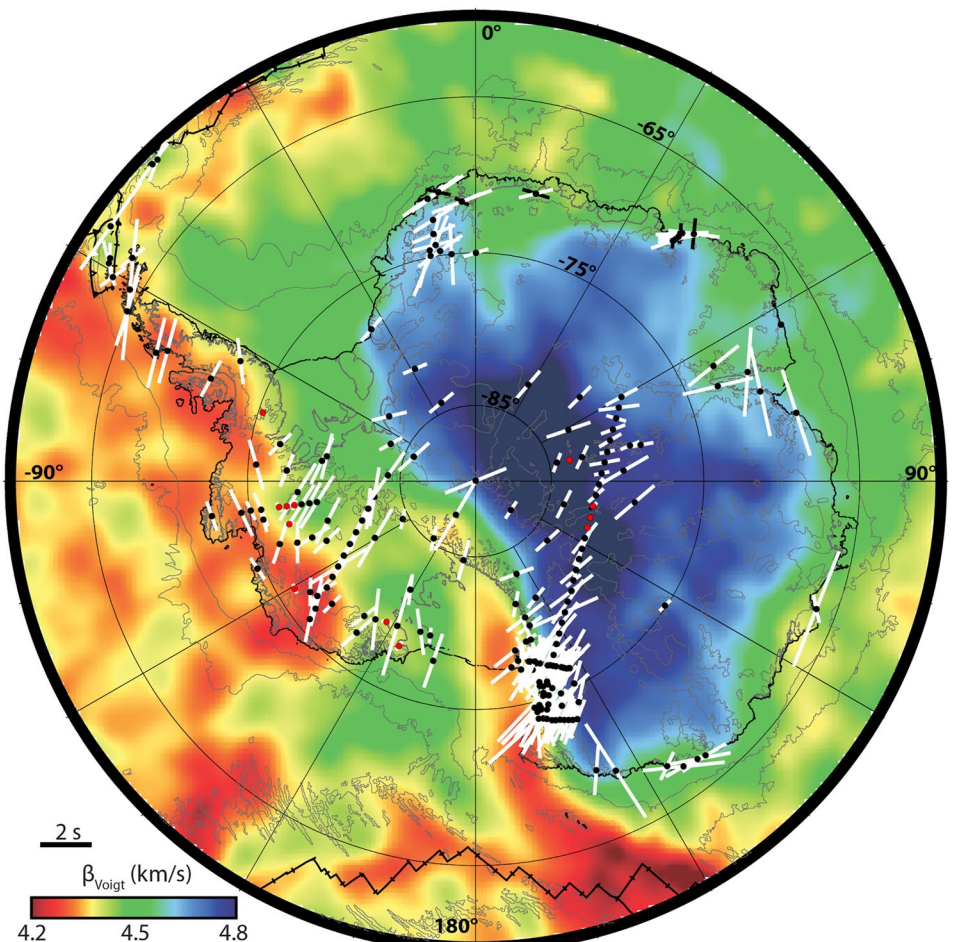


**Figure 6.** Splitting results plotted on the Lloyd et al. (2020) seismic model at 150 km depth. White lines represent results from this study and previous studies. Seismic stations with  $\delta t \geq 0.3$  s and  $\delta t < 0.3$  s are marked with black and red circles, respectively. Two-layer azimuthal anisotropy results, modeled by Müller (2001) and Usui et al. (2007), are plotted with white (upper layer) and black (lower layer) lines.

anisotropy may be interpreted as a fabric that was frozen into the lithosphere before the breakup of Gondwana. Paleomagnetic data indicate the HEW was initially located adjacent to the Pensacola Mountains and Coats Land and rotated  $\sim 90^\circ$  counterclockwise relative to EANT between 230 and 110 Ma (Grunow et al., 1991). Fast polarization directions found in the HEW differ systematically from those found in the Pensacola Mountains and Coats Land (Figures 1 and 3), potentially indicative of an anisotropic fabric frozen into the lithosphere of HEW before its rotation relative to the Pensacola Mountains and Coats Land. This implies that a restoration of the Gondwana supercontinent, maintaining currently observed anisotropy, would bring  $\phi$  directions observed in the HEW, Pensacola Mountains, and Coats Land into alignment. Yet another alternative exists however: as polarization directions throughout the HEW trend approximately orthogonal to the extensional rift fabric of the Southern Weddell Magnetic Province (Jordan et al., 2017; Figure 3), HEW anisotropy could be associated with the Jurassic extension of the Weddell Sea Rift System. NNE-SSW oriented  $\phi$  directions in the southern HEW may be associated, at least in part, with the NNE-SSW striking Pagano Shear Zone, a major left-lateral strike-slip fault system that likely accommodated the southwards motion of the HEW during the Jurassic opening of the Weddell Sea Rift System (Jordan et al., 2013; Figure 3). Notably, the parallelism between  $\phi$  directions and the strike of the Pagano Shear Zone is suggestive of a mechanical coupling between the crust and mantle, similar to that proposed for numerous other shear zones (see Vauchez et al., 2012 for a review).

#### 5.2.2.3. Marie Byrd Land (Figure 3)

As numerous studies provide evidence for an MBL mantle plume (e.g., Emry et al., 2015; LeMasurier & Landis, 1996; Panter et al., 1997; Weaver et al., 1994), upper mantle anisotropy may be attributable to processes associated with a mantle plume beneath MBL. Geodynamic models of anisotropy for typical mantle plumes indicate that  $\phi$  directions should be oriented vertically within the upwelling plume stem, perpendicular to radial flow in the deeper portion of the expanding plume head, and approximately parallel to radial flow in the shallower portion of the expanding plume head (e.g., Druken et al., 2013). In general, splitting measurements in MBL are not consistent with those expected of a classically structured mantle plume; however, as many factors can influence plume flow, such as plate motion and relief at the base of the lithosphere, splitting measurements in MBL may still reflect mantle plume processes.

As suggested by Accardo et al. (2014), MBL anisotropy could alternatively reflect a relict upper mantle fabric developed during the late Cretaceous – early Cenozoic extension of the WARS, before the onset of plume activity. Consistent with a fabric related to WARS extension,  $\phi$  directions are largely oriented sub-parallel to the inferred extensional direction (e.g., Siddoway, 2008; Figure 3). In this case, discrepancies between  $\phi$  directions and the inferred direction of late Cretaceous – early Cenozoic WARS extension observed at several stations throughout MBL may reflect other processes, such as localized Cenozoic extension in WANT or plate motion-induced asthenospheric flow (Figures 3 and 4).

#### 5.2.2.4. AP, South Shetland Islands, and South Orkney Islands (Figure 3)

Upper mantle anisotropy within the contiguous AP likely reflects (a) Permian–Neogene subduction of the Phoenix Plate beneath the AP crustal block (e.g., Dalziel & Elliot, 1982; Storey et al., 1988), (b) tectonic processes associated with the breakup of Gondwana, and/or (c) plate motion-induced asthenospheric flow (Figures 3 and 4). While Helffrich et al. (2002) attributed  $\phi$  directions in the northernmost AP and South Shetland Islands to a single, ocean-basin scale flow field in the South Atlantic, our splitting measurements indicate that anisotropy in the northernmost AP, South Shetland Islands, and South Orkney Islands may instead be attributable to local plate boundary processes (Figures 1–3). Several stations in the South Shetland Islands show  $\phi$  directions oriented approximately perpendicular to the South Shetland Trench and, thus, likely reflect asthenospheric deformation associated with the active subduction zone (Figures 1–3). With  $\phi$  directions oriented sub-parallel to the strike of the Bransfield Strait, splitting measurements at JUBA and FREI likely reflect the asthenospheric fabric of the active rift setting (Figures 1–3). Finally,  $\phi$  directions in the South Orkney Island are perhaps best attributed to asthenospheric shearing associated with the adjacent Antarctic–Scotia plate boundary (Figures 1–3).

#### 5.2.2.5. Thurston Island-Eights Coast Crustal Block (Figure 3)

Anisotropy observed in the TIE, a region underlain by relatively thin lithosphere (Figure 5a), likely reflects both lithospheric and sub-lithospheric fabrics. Fossil anisotropy in TIE may reflect a fabric associated with the Paleozoic – Mesozoic subduction of the proto-Pacific plate along the eastern margin of Gondwana and/or

localized extension in the ASE associated with WARS extension (e.g., Jordan et al., 2010; Luyendyk et al., 2003; Siddoway, 2008). Alternatively, like the HEW, TIE anisotropy may be interpreted as a fabric frozen into the lithosphere before its ~90° counterclockwise rotation away from the Pensacola Mountains and Coats Land between 230 and 110 Ma (Grunow et al., 1991). In addition to relict fabrics frozen into the lithosphere, splitting measurements in the TIE likely reflect sub-lithospheric fabrics, possibly associated with the flow of mantle material away from MBL (Accardo et al., 2014; Figure 6) or APM-induced asthenospheric flow (Figure 4).

#### 5.2.2.6. Northern Transantarctic Mountains (*Figure 3*)

While predominantly Grid NE-SW-oriented  $\phi$  directions are observed across much of the NTAM, Grid N-S and NW-SE oriented  $\phi$  directions are also found in the NTAM. Grid NE-SW-oriented  $\phi$  directions are not likely attributable to the Ross Orogeny, a large compressional tectonic event occurring at ~500 Ma characterized by a NE-SW direction of shortening (Allibone, 1987; Findlay, 1978; Findlay et al., 1984; Stump, 1995) that would presumably produce NW-SE oriented mantle fabric. Previous studies have also attributed Grid NE-SW-oriented  $\phi$  directions to a relict fabric pre-dating the Ross Orogeny (Barklage et al., 2009; Graw & Hansen, 2017). The Grid NE-SW  $\phi$  directions, in addition, trend sub-parallel to the direction of Cretaceous extension in the Ross Sea and, thus may alternatively reflect a relict fabric associated with the initiation of WARS extension in the Ross Sea (Siddoway, 2008). Unlike the Grid NE-SW-oriented  $\phi$  directions, the Grid N-S and NW-SE oriented  $\phi$  directions in the NTAM trend parallel/sub-parallel to the NE-SW direction of shortening characteristic of the Ross Orogeny and may reflect orogen-parallel anisotropy, similar to that found in other mountain ranges. Alternatively, the Grid NW-SE oriented  $\phi$  directions are aligned approximately parallel to APM directions in the NTAM and, thus, could reflect, at least in part, plate motion-induced asthenospheric flow (Figures 3 and 4).

#### 5.2.2.7. Southern Transantarctic Mountains (*Figure 3*)

Largely NW-SE oriented  $\phi$  directions found across the STAM may reflect a fabric developed during the extension of the WARS, a relict fabric pre-dating the Ross Orogeny, and/or active asthenospheric flow (Figures 2 and 3). With an exceptionally large split time (1.6 s) and  $\phi$  oriented perpendicular to the mountain front, the splitting measurement at HOWE may reflect mantle flow resulting from lithospheric foundering observed in tomographic images (Shen et al., 2018) and be associated with nearby Miocene volcanics (Stump et al., 1980; Figures 1–3). The  $\phi$  direction measured at seismic station DUFK (Figure 1), located in the Pensacola Mountains, is oriented approximately normal to the extensional rift fabric of the Southern Weddell Magnetic Province, and is, therefore, likely best attributed to the Jurassic extension of the Weddell Sea Rift System (e.g., Jordan et al., 2017; Figures 2 and 3).

## 6. Summary and Conclusions

In summary, we report 102 new and revised shear wave splitting measurements for continental Antarctica obtained from teleseismic SKS, SKKS, and PKS phases. The ensemble of splitting measurements, including new, revised, and previously published measurements, reveals largely NE-SW-oriented fast polarization directions across Antarctica, with a clockwise rotation in fast polarization directions broadly evident moving from west to east across the continent. Somewhat higher magnitude splitting times, on average, are generally found in regions associated with recent tectonic activity and thinner lithosphere, whereas somewhat lower magnitude splitting times are found in regions characterized by prolonged tectonic quiescence and thick lithosphere; however, significant scatter exists in the splitting times within regions of both thicker and thinner lithosphere.

While NE-SW-oriented fast polarization directions are found across much of Antarctica, the observed anisotropy cannot reasonably be attributed to a single plate-wide source, such as fossil anisotropy, plate-scale mantle flow, or a combination of small-scale flow regimes in the mantle. We therefore attribute the shear wave splitting patterns to different sources in different regions of Antarctica, taking into consideration the tectonic history of known terranes. Upper mantle anisotropy likely reflects primarily relict lithospheric fabrics in regions underlain by thick lithosphere, such as central EANT and the HEW, while anisotropy observed elsewhere likely reflects both lithospheric and sub-lithospheric fabrics associated with a number of sources, including relict fabrics in the mantle lithosphere, plate motion-induced asthenospheric flow, and small-scale convection. Overall, we conclude that the observed upper mantle anisotropy likely arises from regionally variable contributions of lithospheric and sub-lithospheric sources across Antarctica.

## Data Availability Statement

All seismic data utilized in this study can be obtained from the IRIS Data Management Center ([www.iris.edu](http://www.iris.edu)). Figures in this study were made using the Generic Mapping Tools (Wessel et al., 2019). The SplitLab software package is available at <http://splitting.gm.univ-montp2.fr>. The authors thank Ray Russo and an anonymous reviewer for their helpful and constructive comments.

## Acknowledgments

This work was supported by the National Science Foundation (NSF) (Grants 1142126, 1142518, 1141916, 1148982, 1246416, 1246151, 1249631, 1249602, 1249513, 1246666, 1246712, 1246776, and 1247518) and by the Natural Environment Research Council (Grants NE/L006065/1, NE/L006294/1, and NE/K009958/1). POLENET/ANET seismic instrumentation was provided and supported by the Incorporated Research Institutions for Seismology (IRIS) through the Portable Array Seismic Studies of the Continental Lithosphere (PASSCAL) Instrument Center at New Mexico Tech. UKANET seismic instrumentation was provided and supported by SEIS-UK.

## References

- Accardo, N. J., Wiens, D. A., Hernandez, S., Aster, R. C., Nyblade, A. A., Huerta, A., et al. (2014). Upper mantle seismic anisotropy beneath the West Antarctic Rift System and surrounding region from shear wave splitting analysis. *Geophysical Journal International*, 198(1), 414–429. <https://doi.org/10.1093/gji/ggu117>
- Allibone, A. (1987). Koettlitz Group metasediments and orthogneisses from the mid Taylor Valley and Ferrar Glacier areas. *New Zealand Antarctic Record*, 8(1), 48–60.
- An, M., Wiens, D. A., Zhao, Y., Feng, M., Nyblade, A., Kanao, M., et al. (2015). S-velocity model and inferred Moho topography beneath the Antarctic Plate from Rayleigh waves. *Journal of Geophysical Research: Solid Earth*, 120, 359–383. <https://doi.org/10.1002/2014JB011332>
- Baranov, A., Tenszer, R., & Morelli, A. (2021). Updated Antarctic crustal model. *Gondwana Research*, 89, 1–18. <https://doi.org/10.1016/j.gr.2020.08.010>
- Barker, P. F. (1982). The Cenozoic subduction history of the Pacific margin of the Antarctic Peninsula: Ridge crest–trench interactions. *Journal of the Geological Society*, 139, 787–801. <https://doi.org/10.1144/gsjgs.139.6.0787>
- Barklage, M., Wiens, D. A., Nyblade, A., & Anandakrishnan, S. (2009). Upper mantle seismic anisotropy of South Victoria Land and the Ross Sea coast, Antarctica from SKS and SKKS splitting analysis. *Geophysical Journal International*, 178, 729–741. <https://doi.org/10.1111/j.1365-246X.2009.04158.x>
- Bayer, B., Geissler, W. H., Eckstaller, A., & Jokat, W. (2009). Seismic imaging of the crust beneath Dronning Maud Land, East Antarctica. *Geophysical Journal International*, 178(2), 860–876. <https://doi.org/10.1111/j.1365-246X.2009.04196.x>
- Bayer, B., Müller, C., Eaton, D. W., & Jokat, W. (2007). Seismic anisotropy beneath Dronning Maud Land, Antarctica, revealed by shear wave splitting. *Geophysical Journal International*, 171, 339–351. <https://doi.org/10.1111/j.1365-246X.2007.03519.x>
- Becker, T. W., & Boschi, L. (2002). A comparison of tomographic and geodynamic mantle models. *Geochemistry, Geophysics, Geosystems*, 3, 1003. <https://doi.org/10.1029/2001GC000168>
- Becker, T. W., & O'Connell, R. J. (2001). Predicting plate velocities with mantle circulation models. *Geochemistry, Geophysics, Geosystems*, 2, 1060. <https://doi.org/10.1029/2001GC000171>
- Behrendt, J. C., & Cooper, A. (1991). Evidence of rapid Cenozoic uplift of the shoulder escarpment of the Cenozoic West Antarctic rift system and a speculation on possible climate forcing. *Geology*, 19(4), 315–319. [https://doi.org/10.1130/0091-7613\(1991\)019<0315:EORCUO>2.3.CO;2](https://doi.org/10.1130/0091-7613(1991)019<0315:EORCUO>2.3.CO;2)
- Bernard, R. E., Behr, W. M., Becker, T. W., & Young, D. J. (2019). Relationships between olivine CPO and deformation parameters in naturally deformed rocks and implications for mantle seismic anisotropy. *Geochemistry, Geophysics, Geosystems*, 20, 3469–3494. <https://doi.org/10.1029/2019GC008289>
- Bird, P. (2003). An updated digital model of plate boundaries. *Geochemistry, Geophysics, Geosystems*, 4(3), 1027. <https://doi.org/10.1029/2001GC000252>
- Boger, S. D. (2011). Antarctica – Before and after Gondwana. *Gondwana Research*, 19, 335–371. <https://doi.org/10.1016/j.gr.2010.09.003>
- Boger, S. D., Carson, C. J., Fanning, C. M., Hergt, J. M., Wilson, C. J. L., & Woodhead, J. D. (2002). Pan-African intraplate deformation in the northern Prince Charles Mountains, East Antarctica. *Earth and Planetary Science Letters*, 195, 195–210. [https://doi.org/10.1016/S0012-821X\(01\)00587-8](https://doi.org/10.1016/S0012-821X(01)00587-8)
- Brenn, G. R., Hansen, S. E., & Park, Y. (2017). Variable thermal loading and flexural uplift along the Transantarctic Mountains, Antarctica. *Geology*, 45(5), 463–466. <https://doi.org/10.1130/G38784.1>
- Chatzaras, V., & Kruckenberg, S. C. (2021). *Effects of melt-percolation, refertilization and deformation on upper mantle seismic anisotropy: Constraints from peridotite xenoliths*. (Vol. 56). Geological Society London Memoirs. <https://doi.org/10.1144/M56-2020-16>
- Dalziel, I. W. D. (1992). Antarctica; A tale of two supercontinents? *Annual Review of Earth and Planetary Sciences*, 20(1), 501–526. <https://doi.org/10.1146/annurev.ea.20.050192.002441>
- Dalziel, I. W. D. (2007). *The Ellsworth Mountains: Critical and enduringly enigmatic. Paper presented at International Symposium on Antarctic Earth Sciences*. U.S. Geological Survey and The National Academies. USGS OF-2007-1047, Short Research Paper 004. <https://doi.org/10.3133/of2007-1047.srp004>
- Dalziel, I. W. D., & Elliot, D. H. (1982). West Antarctica: Problem child of Gondwanaland. *Tectonics*, 1(1), 3–19. <https://doi.org/10.1029/tc001i001p00003>
- Druken, K. A., Kincaid, C., & Griffiths, R. W. (2013). Directions of seismic anisotropy in laboratory models of mantle plumes. *Geophysical Research Letters*, 40, 3544–3549. <https://doi.org/10.1002/grl.50671>
- Dunham, C. K., O'Donnell, J. P., Stuart, G. W., Brisbourne, A. M., Rost, S., Jordan, T. A., et al. (2020). A joint inversion of receiver function and Rayleigh wave phase velocity dispersion data to estimate crustal structure in West Antarctica. *Geophysical Journal International*, 223(3), 1644–1657. <https://doi.org/10.1093/gji/ggaa398>
- Emry, E. L., Nyblade, A. A., Julià, J., Anandakrishnan, S., Aster, R. C., Wiens, D. A., et al. (2015). The mantle transition zone beneath West Antarctica: Seismic evidence for hydration and thermal upwellings. *Geochemistry, Geophysics, Geosystems*, 16(1), 40–58. <https://doi.org/10.1002/2014gc005588>
- Faccenna, C., Rossetti, F., Becker, T. W., Danesi, S., & Morelli, A. (2008). Recent extension driven by mantle upwelling beneath the Admiralty Mountains (East Antarctica). *Tectonics*, 27(4). <https://doi.org/10.1029/2007TC002197>
- Ferraccioli, F., Finn, C. A., Jordan, T. A., Bell, R. E., Anderson, L. M., & Damaske, D. (2011). East Antarctic rifting triggers uplift of the Gamburtsev Mountains. *Nature*, 479, 388–392. <https://doi.org/10.1038/nature10566>
- Findlay, R. H. (1978). Provisional report on the geology of the region between the Renegar and Blue Glaciers, Antarctica. *New Zealand Antarctic Record*, 1, 29–44.
- Findlay, R. H., Craw, D., & Skinner, D. N. B. (1984). Lithostratigraphy and structure of the Koettlitz Group, McMurdo Sound, Antarctica. *New Zealand Journal of Geology and Geophysics*, 27(4), 513–536. <https://doi.org/10.1080/00288306.1984.10422270>

- Finn, C. A., Müller, R. D., & Panter, K. S. (2005). A Cenozoic diffuse alkaline magmatic province (DAMP) in the southwest Pacific without rift or plume origin. *Geochemistry, Geophysics, Geosystems*, 6, Q02005. <https://doi.org/10.1029/2004GC000723>
- Fitzgerald, P. G. (2002). Tectonics and landscape evolution of the Antarctic plate since Gondwana breakup, with an emphasis on the West Antarctic rift system and the Transantarctic Mountains. In J. Gamble, D. Skinner, & S. Henrys (Eds.), *Antarctica at the Close of a Millennium. Proceedings of the 8th International Symposium on Antarctic Earth Science* (Vol. 35, pp. 453–469). The Royal Society of New Zealand.
- Fitzgerald, P. G., & Stump, E. (1991). Early Cretaceous uplift of the Ellsworth Mountains, West Antarctica. *Science*, 254, 92–94.
- Fitzsimons, I. C. W. (2000a). A review of tectonic events in the East Antarctic Shield, and their implications for Gondwana and earlier supercontinents. *Journal of African Earth Sciences*, 31, 3–23.
- Fitzsimons, I. C. W. (2000b). Grenville aged basement provinces in East Antarctica: Evidence for three separate collisional orogens. *Geology*, 28, 879–882.
- Fitzsimons, I. C. W. (2003). Proterozoic basement provinces of southwestern Australia, and their correlation with Antarctica. In Y. Yoshida, B. F. Windley, & S. Dasgupta (Eds.), *Proterozoic East Gondwana: Supercontinent assembly and breakup* (Vol. 206, pp. 93–130). Special Publications Geological Society. <https://doi.org/10.1144/GSL.SP.2003.206.01.07>
- Ford, A. B. (1972). Weddell orogeny—Latest Permian to early Mesozoic deformation at the Weddell Sea margin of the Transantarctic Mountains. In R. J. Adie (Ed.), *Antarctic Geology and Geophysics* (pp. 419–425).
- Fouch, M. J., & Rondenay, S. (2006). Seismic anisotropy beneath stable continental interiors. *Physics of the Earth and Planetary Interiors*, 158, 292–320. [doi:10.1016/j.pepi.2006.03.024](https://doi.org/10.1016/j.pepi.2006.03.024)
- Golynsky, A. V., Ferraccioli, F., Hong, J. K., Golynsky, D. A., von Frese, R. R. B., Young, D. A., et al. (2018). New magnetic anomaly map of the Antarctic. *Geophysical Research Letters*, 45, 6437–6449. <https://doi.org/10.1029/2018GL078153>
- Goodge, J. W. (2020). Geological and tectonic evolution of the Transantarctic Mountains, from ancient craton to recent enigma. *Gondwana Research*, 80, 50–122. <https://doi.org/10.1016/j.gr.2019.11.001>
- Goodge, J. W., & Fanning, C. M. (2016). Mesoproterozoic and Paleoproterozoic history of the Nimrod complex, central Transantarctic Mountains, Antarctica: Stratigraphic revisions and relation to the Mawson Continent in East Gondwana. *Precambrian Research*, 285, 242–271. <https://doi.org/10.1016/j.precamres.2016.09.001>
- Granot, R., Cande, S. C., Stock, J. M., & Damaske, D. (2013). Revised Eocene-Oligocene kinematics for the West Antarctic rift system. *Geophysical Research Letters*, 40, 279–284. <https://doi.org/10.1029/2012GL054181>
- Granot, R., Cande, S. C., Stock, J. M., Davey, F. J., & Clayton, R. W. (2010). Postspreading rifting in the Adare Basin, Antarctica: Regional tectonic consequences. *Geochemistry, Geophysics, Geosystems*, 11(8). <https://doi.org/10.1029/2010GC003105>
- Graw, J. H., Adams, A. N., Hansen, S. E., Wiens, D. A., Hackworth, L., & Park, Y. (2016). Upper mantle shear wave velocity structure beneath northern Victoria land, Antarctica: Volcanism and uplift in the northern Transantarctic Mountains. *Earth and Planetary Science Letters*, 449, 48–60. <https://doi.org/10.1016/j.epsl.2016.05.026>
- Graw, J. H., & Hansen, S. E. (2017). Upper mantle seismic anisotropy beneath the Northern Transantarctic Mountains, Antarctica from PKS, SKS, and SKKS splitting analysis. *Geochemistry, Geophysics, Geosystems*, 18, 544–557. <https://doi.org/10.1002/2016GC006729>
- Gripp, A. E., & Gordon, R. G. (2002). Young tracks of hotspots and current plate velocities. *Geophysical Journal International*, 150, 321–361. <https://doi.org/10.1046/j.1365-246X.2002.01627.x>
- Grunow, A. M., Kent, D. V., & Dalziel, I. W. D. (1991). New paleomagnetic data from Thurston Island: Implications for the tectonics of West Antarctica and Weddell Sea opening. *Journal of Geophysical Research: Solid Earth*, 96(B11). <https://doi.org/10.1029/91JB01507>
- Hansen, S. E., Graw, J. H., Kenyon, L. M., Nyblade, A. A., Wiens, D. A., Aster, R. C., et al. (2014). Imaging the Antarctic mantle using adaptively parameterized P-wave tomography: Evidence for heterogeneous structure beneath west Antarctica. *Earth and Planetary Science Letters*, 408, 66–78. <https://doi.org/10.1016/j.epsl.2014.09.043>
- Hansen, S. E., Kenyon, L. M., Graw, J. H., Park, Y., & Nyblade, A. A. (2016). Crustal structure beneath the Northern Transantarctic Mountains and Wilkes subglacial basin: Implications for tectonic origins. *Journal of Geophysical Research: Solid Earth*, 121, 812–825. <https://doi.org/10.1002/2015JB012325>
- Hansen, S. E., Nyblade, A. A., Heeszel, D. S., Wiens, D. A., Shore, P., & Kanao, M. (2010). Crustal structure of the Gamburtsev Mountains, East Antarctica, from S-wave receiver functions and Rayleigh wave phase velocities. *Earth and Planetary Science Letters*, 300, 395–401. <https://doi.org/10.1016/j.epsl.2010.10.022>
- Harley, S. L., Fitzsimons, I. C. W., & Zhao, Y. (2013). Antarctica and supercontinent evolution: Historical perspectives, recent advances and unresolved issues. *Geological Society London*, 383, 1–34. <https://doi.org/10.1144/SP383.9>
- Heeszel, D. S., Wiens, D. A., Anandakrishnan, S., Aster, R. C., Dalziel, I. W., Huerta, A. D., et al. (2016). Upper mantle structure of central and West Antarctica from array analysis of Rayleigh wave phase velocities. *Journal of Geophysical Research: Solid Earth*, 121, 1758–1775. <https://doi.org/10.1002/2015JB012616>
- Heeszel, D. S., Wiens, D. A., Nyblade, A. A., Hansen, S. E., Kanao, M., An, M., & Zhao, Y. (2013). Rayleigh wave constraints on the structure and tectonic history of the Gamburtsev Subglacial Mountains, East Antarctica. *Journal of Geophysical Research: Solid Earth*, 118, 2138–2153. <https://doi.org/10.1002/jgrb.50171>
- Helffrich, G., Wiens, D. A., Vera, E., Barrientos, S., Shore, P., Robertson, S., & Adarov, R. (2002). A teleseismic shear-wave splitting study to investigate mantle flow around South America and implications for plate-driving forces. *Geophysical Journal International*, 149, F1–F7. <https://doi.org/10.1046/j.1365-246X.2002.01636.x>
- Hernandez, S., Wiens, D., Anandakrishnan, S., Aster, R., Huerta, A., Nyblade, A., & Wilson, T. (2009). Seismic anisotropy of the Antarctic upper mantle from shear wave splitting analysis of POLENET and AGAP seismograms. *Eos Transactions American Geophysical Union, Fall Meeting Supplement*.
- Jacobs, J., Fanning, C. M., Henjes-Kunst, F., Olesch, M., & Paech, H.-J. (1998). Continuation of the Mozambique Belt into East Antarctica: Grenville-age metamorphism and polyphase Pan-African high-grade events in Central Dronning Maud Land. *The Journal of Geology*, 106(4). <https://doi.org/10.1086/516031>
- Jordan, T. A., Ferraccioli, F., & Leat, P. T. (2017). New geophysical compilations link crustal block motion to Jurassic extension and strike-slip faulting in the Weddell Sea Rift System of West Antarctica. *Gondwana Research*, 42, 29–48. <https://doi.org/10.1016/j.gr.2016.09.009>
- Jordan, T. A., Ferraccioli, F., Ross, N., Corr, H. F., Leat, P. T., Bingham, R. G., et al. (2013). Inland extent of the Weddell Sea Rift imaged by new aerogeophysical data. *Tectonophysics*, 585, 137–160. <https://doi.org/10.1016/j.tecto.2012.09.010>
- Jordan, T. A., Ferraccioli, F., Vaughan, D. G., Holt, J. W., Corr, H., Blankenship, D. D., & Diehl, T. M. (2010). Aerogravity evidence for major crustal thinning under the Pine Island glacier region (West Antarctica). *Bulletin of the Geological Society of America*, 122(5–6), 714–726. <https://doi.org/10.1130/B26417.1>
- Jordan, T. A., Riley, T. R., & Siddoway, C. S. (2020). The geological history and evolution of West Antarctica. *Nature Reviews Earth Environment*, 1, 117–133. <https://doi.org/10.1038/s43017-019-0013-6>

- Karato, S., Jung, H., Katayama, I., & Skemer, P. (2008). Geodynamic significance of seismic anisotropy of the upper mantle: New insights from laboratory studies. *Annual Review of Earth and Planetary Sciences*, 36, 59–95. <https://doi.org/10.1146/annurev.earth.36.031207.124120>
- Karato, S., & Wu, P. (1993). Rheology of the upper mantle: A synthesis. *Science*, 260(5109), 771–778. <https://doi.org/10.1126/science.260.5109.771>
- King, S. D., & Anderson, D. L. (1998). Edge-driven convection. *Earth and Planetary Science Letters*, 160(3–4), 289–296. [https://doi.org/10.1016/S0012-821X\(98\)00089-2](https://doi.org/10.1016/S0012-821X(98)00089-2)
- Kubo, A., Hiramatsu, Y., Kanao, M., Ando, M., & Terashima, T. (1995). An analysis of the SKS splitting at Syowa station in Antarctica. *Proceedings of the NIPR Symposium on Antarctic Geosciences*, 8, 25–34.
- Lamarque, G., Barruol, G., Fontaine, F. R., Bascou, J., & Ménot, R.-P. (2015). Crustal and mantle structure beneath the Terre Adélie Craton, East Antarctica: Insights from receiver function and seismic anisotropy measurements. *Geophysical Journal International*, 200(2), 807–821. <https://doi.org/10.1093/gji/ggu430>
- Larter, R. D., & Barker, P. F. (1991). Effects of ridge crest-trench interaction on Antarctic-Phoenix Spreading: Forces on a young subducting plate. *Journal of Geophysical Research*, 96(B12), 19583–19607. <https://doi.org/10.1029/91JB02053>
- LeMasurier, W. E., & Landis, C. A. (1996). Mantle-plume activity recorded by low-relief erosion surfaces in West Antarctica and New Zealand. *The Geological Society of America Bulletin*, 108(11), 1450–1466. [https://doi.org/10.1130/0016-7606\(1996\)108<1450:MPARBL>2.3.CO;2](https://doi.org/10.1130/0016-7606(1996)108<1450:MPARBL>2.3.CO;2)
- Lloyd, A. J., Nyblade, A. A., Wiens, D. A., Shore, P. J., Hansen, S. E., Kanao, M., & Zhao, D. (2013). Upper mantle seismic structure beneath central East Antarctica from body wave tomography: Implications for the origin of the Gamburtsev Subglacial Mountains. *Geochemistry, Geophysics, Geosystems*, 14(4), 902–920. <https://doi.org/10.1002/ggge.20098>
- Lloyd, A. J., Wiens, D. A., Nyblade, A. A., Anandakrishnan, S., Aster, R. C., Huerta, A. D., et al. (2015). A seismic transect across West Antarctica: Evidence for mantle thermal anomalies beneath the Bentley Subglacial Trench and the Marie Byrd Land Dome. *Journal of Geophysical Research: Solid Earth*, 120(12), 8439–8460. <https://doi.org/10.1002/2015jb012455>
- Lloyd, A. J., Wiens, D. A., Zhu, H., Tromp, J., Nyblade, A. A., Aster, R. C., et al. (2020). Seismic structure of the Antarctic upper mantle based on adjoint tomography. *Journal of Geophysical Research: Solid Earth*, 124. <https://doi.org/10.1029/2019JB017823>
- Llubes, M., Seoane, L., Bruinsma, S., & Rémy, F. (2018). Crustal thickness of Antarctica estimated using data from gravimetric satellites. *Solid Earth*, 9, 457–467. <https://doi.org/10.5194/se-9-457-2018>
- Loewy, S. L., Dalziel, I. W. D., Pisarevsky, S., Connelly, J. N., Tait, J., Hanson, R. E., & Bullen, D. (2011). Coats Land crustal block, East Antarctica: A tectonic tracer for Laurentia? *Geology*, 39(9), 859–862. <https://doi.org/10.1130/G32029.1>
- Long, M. D., & Silver, P. G. (2009). Shear wave splitting and mantle anisotropy: Measurements, interpretations, and new directions. *Surveys in Geophysics*, 30, 407–461. <https://doi.org/10.1007/s10712-009-9075-1>
- Lucas, E. M., Nyblade, A. A., Lloyd, A. J., Aster, R. C., Wiens, D. A., O'Donnell, J. P., et al. (2021). Seismicity and Pn velocity structure of Central West Antarctica. *Geochemistry, Geophysics, Geosystems*, 22, e2020GC009471. <https://doi.org/10.1029/2020GC009471>
- Lucas, E. M., Soto, D., Nyblade, A. A., Lloyd, A. L., Aster, R. C., Wiens, D. A., et al. (2020). P- and S-wave velocity structure of central West Antarctica: Implications for the tectonic evolution of the West Antarctic Rift System. *Earth and Planetary Science Letters*, 546. <https://doi.org/10.1016/j.epsl.2020.116437>
- Luyendyk, B. P., Wilson, D. S., & Siddoway, C. S. (2003). Eastern margin of the Ross Sea Rift in Western Marie Byrd Land, Antarctica: Crustal structure and tectonic development. *Geochemistry, Geophysics, Geosystems*, 4, 1090. <https://doi.org/10.1029/2002GC000462>
- Mainprice, D., Barruol, G., & Ben Ismaïl, W. (2000). The seismic anisotropy of the Earth's mantle: From single crystal to polycrystal. In S.-I. Karato, A. Forte, R. Liebermann, G. Masters, & L. Stixrude (Eds.), *Earth's deep interior: Mineral physics and tomography from the atomic to the global scale*, *Geophysical Monograph Series* (Vol. 117). American Geophysical Union.
- Mainprice, D., Tommasi, A., Couvy, H., Cordier, P., & Frost, D. J. (2005). Pressure sensitivity of olivine slip systems: Implications for the interpretation of seismic anisotropy of the Earth's upper mantle. *Nature*, 433, 731–733. <https://doi.org/10.1038/nature03266>
- Meert, J. G. (2003). A synopsis of events related to the assembly of eastern Gondwana. *Tectonophysics*, 362, 1–40. [https://doi.org/10.1016/S0040-1951\(02\)00629-7](https://doi.org/10.1016/S0040-1951(02)00629-7)
- Ménot, R., Duclaux, G., Peucat, J. J., Rolland, Y., Guillot, S., Fanning, M., et al. (2007). Geology of the Terre Adélie Craton (135–146°E). In A. K. Cooper, C. R. Raymond, & ISAES Editorial Team (Eds.), *Antarctica: A Keystone in a Changing World – Online Proceedings of the 10th ISAES USGS Open-File Report 2007-1047*, Short Research Paper 048, 5 p. <https://doi.org/10.3133/of2007-1047.srp048>
- Morlighem, M., Rignot, E., Binder, T., Blankenship, D., Drews, R., Eagles, G., et al. (2020). Deep glacial troughs and stabilizing ridges unveiled beneath the margins of the Antarctic ice sheet. *Nature Geoscience*, 13, 132–137. <https://doi.org/10.1038/s41561-019-0510-8>
- Müller, C. (2001). Upper mantle seismic anisotropy beneath Antarctica and the Scotia Sea region. *Geophysical Journal International*, 147, 105–122. <https://doi.org/10.1046/j.1365-246X.2001.00517.x>
- Nicolas, A. (1993). Why fast polarization directions of SKS seismic waves are parallel to mountain belts. *Physics of the Earth and Planetary Interiors*, 78, 337–342. [https://doi.org/10.1016/0031-9201\(93\)90164-5](https://doi.org/10.1016/0031-9201(93)90164-5)
- Nicolas, A., & Christensen, N. I. (1987). Formation of anisotropy in upper mantle peridotites – A Review. In K. Fuchs, & C. Froidevaux (Eds.), *Composition, structure and dynamics of the lithosphere-asthenosphere system*, *Geodynamics Series* (Vol. 16, pp. 111–123). American Geophysical Union.
- O'Donnell, J. P., & Nyblade, A. A. (2014). Antarctica's hypsometry and crustal thickness: Implications for the origin of anomalous topography in East Antarctica. *Earth and Planetary Science Letters*, 388, 143–155. <https://doi.org/10.1016/j.epsl.2013.11.051>
- O'Donnell, J. P., Stuart, G. W., Brisbourne, A. M., Selway, K., Yang, Y., & Nield, G. A. (2019). The uppermost mantle seismic velocity structure of West Antarctica from Rayleigh wave tomography: Insights into tectonic structure and geothermal heat flow. *Earth and Planetary Science Letters*, 522, 219–233. <https://doi.org/10.1016/j.epsl.2019.06.024>
- Panter, K. S., Kyle, P. R., & Smellie, J. L. (1997). Petrogenesis of a phonolite-trachyte succession at Mount Sidley, Marie Byrd Land, Antarctica. *Journal of Petrology*, 38(9), 1225–1253.
- Phillips, E. H., Sims, K. W. W., Blachert-Toft, J., Aster, R. C., Gaetani, G. A., Kyle, P. R., et al. (2018). The nature and evolution of mantle upwelling at Ross Island, Antarctica, with implications for the source of HIMU lavas. *Earth and Planetary Science Letters*, 498, 38–53. <https://doi.org/10.1016/j.epsl.2018.05.049>
- Phillips, G., & Läufer, A. L. (2009). Brittle deformation relating to the Carboniferous–Cretaceous evolution of the Lambert Graben, East Antarctica: A precursor for Cenozoic relief development in an intraplate and glaciated region. *Tectonophysics*, 471(3–4), 216–224. <https://doi.org/10.1016/j.tecto.2009.02.012>
- Pierce, E. L., Hemming, S. R., Williams, T., van de Flierdt, T., Thomson, S. N., Reiners, P. W., et al. (2014). A comparison of detrital U–Pb zircon, 40Ar/39Ar hornblende, 40Ar/39Ar biotite ages in marine sediments off East Antarctica: Implications for the geology of subglacial terrains and provenance studies. *Earth-Science Reviews*, 138, 156–178. <https://doi.org/10.1016/j.earscirev.2014.08.010>
- Podolefsky, N. S., Zhong, S., & McNamara, A. K. (2004). The anisotropic and rheological structure of the oceanic upper mantle from a simple model of plate shear. *Geophysical Journal International*, 158(1), 287–296. <https://doi.org/10.1111/j.1365-246X.2004.02250.x>

- Pondrelli, S., Margheriti, L., & Danesi, S. (2005). Seismic anisotropy beneath Northern Victoria Land from SKS splitting analysis. In D. K.Fütterer, D.Damaske, G.Kleinschmidt, H.Miller, & F.Tessensohn (Eds.), *Antarctica: Contributions to global Earth sciences* (pp. 153–160). Springer.
- Pyle, M., Wiens, D. A., Nyblade, A. A., & Anandakrishnan, S. (2010). Crustal structure of the Transantarctic Mountains near the Ross Sea from ambient seismic noise tomography. *Journal of Geophysical Research*, 115, B11310. <https://doi.org/10.1029/2009JB007081>
- Randall, D. E., & Mac Niocaill, C. (2004). Cambrian palaeomagnetic data confirm a Natal Embayment location for the Ellsworth—Whitmore Mountains, Antarctica. Gondwana reconstructions. *Geophysical Journal International*, 157(1), 105–116. <https://doi.org/10.1111/j.1365-246X.2004.02192.x>
- Reading, A. M., & Heintz, M. (2008). Seismic anisotropy of East Antarctica from shear-wave splitting: Spatially varying contributions from lithospheric structural fabric and mantle flow? *Earth and Planetary Science Letters*, 268, 433–443. <https://doi.org/10.1016/j.epsl.2008.01.041>
- Salimbeni, S., Pondrelli, S., Danesi, S., & Morelli, A. (2010). Seismic anisotropy of the Victoria Land region, Antarctica. *Geophysical Journal International*, 182, 421–432. <https://doi.org/10.1111/j.1365-246X.2010.04624.x>
- Savage, M. K. (1999). Seismic anisotropy and mantle deformation: What have we learned from shear wave splitting? *Reviews of Geophysics*, 37(1), 65–106. <https://doi.org/10.1029/98RG02075>
- Schoopf, J. M. (1969). Ellsworth Mountains: Position in West Antarctica due to seafloor spreading. *Science*, 164, 63–66.
- Shen, W., Wiens, D. A., Anandakrishnan, A., Aster, R. C., Gerstoft, P., Bromirski, P., et al. (2018). The crust and upper mantle structure of central and West Antarctica from Bayesian inversion of Rayleigh wave and receiver functions. *Journal of Geophysical Research*, 123. <https://doi.org/10.1029/2017JB015346>
- Siddoway, C. S. (2008). Tectonics of the West Antarctic Rift System: New light on the history and dynamics of distributed intracontinental extension. In A. K.Cooper, P.Barrett, H.Stagg, B.Storey, E.Stump, W.Wise (Eds.), & the 10th ISAES editorial team(Eds.), *Antarctica: A keystone in a changing world* (pp. 91–114). National Academies Press.
- Sieminski, A., Debye, E., & Leveque, J.-J. (2003). Seismic evidence for deep low-velocity anomalies in the transition zone beneath West Antarctica. *Earth and Planetary Science Letters*, 216, 645–661. [https://doi.org/10.1016/S0012-821X\(03\)00518-1](https://doi.org/10.1016/S0012-821X(03)00518-1)
- Silver, P. G. (1996). Seismic anisotropy beneath the continents: Probing the depths of geology. *Annual Review of Earth and Planetary Sciences*, 24, 385–432. <https://doi.org/10.1146/annurev.earth.24.1.385>
- Silver, P. G., & Chan, W. W. (1991). Shear wave splitting and subcontinental mantle deformation. *Journal of Geophysical Research*, 96, 16429–16454. <https://doi.org/10.1029/91JB00899>
- Silver, P. G., & Savage, M. K. (1994). The interpretation of shear wave splitting parameters in the presence of two anisotropic layers. *Geophysical Journal International*, 119, 949–963. <https://doi.org/10.1029/2003GL017390>
- Stern, T. A., & ten Brink, U. S. (1989). Flexural uplift of the Transantarctic Mountains. *Journal of Geophysical Research*, 94, 10315–10330.
- Storey, B. C., Hole, M. J., Pankhurst, R. J., Millar, I. L., & Vennum, W. R. (1988). Middle Jurassic within-plate granites in West Antarctica and their bearing on the break-up of Gondwanaland. *Journal of the Geological Society*, 145, 999–1007. <https://doi.org/10.1144/gsjgs.145.6.0999>
- Storey, B. C., Macdonald, D. I. M., Dalziel, I. W. D., Isbell, J. L., & Millar, I. L. (1996). Early Paleozoic sedimentation, magmatism, and deformation in the Pensacola Mountains, Antarctica: The significance of the Ross orogeny. *GSA Gulletin*, 108(6), 685–707. [https://doi.org/10.1111/0016-7606\(1996\)108<685:EPSMAD>2.3.CO;2](https://doi.org/10.1111/0016-7606(1996)108<685:EPSMAD>2.3.CO;2)
- Stump, E. (1995). *The Ross Orogen of the Transantarctic Mountains*. Cambridge University Press. pp 284.
- Stump, E., Sheridan, M. F., Borg, S. G., & Sutter, J. F. (1980). Early Miocene subglacial basalts, the East Antarctic ice sheet, and uplift of the Transantarctic Mountains. *Science*, 207, 757–759. <https://doi.org/10.1126/science.207.4432.757>
- Tabacco, I. E., Cianfarra, P., Forieri, A., Salvini, F., & Zirizzotti, A. (2006). Physiography and tectonic setting of the subglacial lake district between Vostok and Belgica subglacial highlands (Antarctica). *Geophysical Journal International*, 165(3), 1029–1040. <https://doi.org/10.1111/j.1365-246X.2006.02954.x>
- Teanby, N. A., Kendall, J. M., & Van Der Baan, M. (2004). Automation of shear-wave splitting measurements using cluster analysis. *Bulletin of the Seismological Society of America*, 94(2), 453–463. <https://doi.org/10.1785/0120030123>
- ten Brink, U. S., Hackney, R. I., Bannister, S., Stern, T. A., & Makovsky, Y. (1997). Uplift of the Transantarctic Mountains and the bedrock beneath the East Antarctic ice sheet. *Journal of Geophysical Research*, 102, 27603–27621.
- Tingeay, R. J. (1991). The regional geology of Archaean and Proterozoic rocks in Antarctica. In R. J.Tingeay (Ed.), *The geology of Antarctica* (pp. 1–73). Oxford University Press.
- Torsvik, T. H., Gaina, C., & Refield, T. F. (2008). Antarctica and global paleogeography: From Rodinia, through Gondwanaland and Pangea, to the birth of the Southern Ocean and the opening of gateways. In A. K. Cooper, C. R., Raymond, & ISAES Editorial Team. (Eds.), *Antarctica: A keystone in a changing world* (pp. 125–140). National Academy of Sciences.
- Usui, Y., Kanao, M., Kubo, A., Hiramatsu, Y., & Negishi, H. (2007). Upper mantle anisotropy from teleseismic SKS splitting beneath Lützow-Holm Bay region, East Antarctica. In A. K. Copper, C. R. Raymond, & ISAES Editorial Team (Eds.), *A Keystone in a Changing World – Online Proceedings of the 10th ISAES*, Open-File report, Short Research Paper 013, 4 p.
- Vauchez, A., & Nicolas, A. (1991). Mountain building: Strike-parallel motion and mantle anisotropy. *Tectonophysics*, 185(3–4), 183–201. [https://doi.org/10.1016/0040-1951\(91\)90443-V](https://doi.org/10.1016/0040-1951(91)90443-V)
- Vauchez, A., Tommasi, A., & Mainprice, D. (2012). Faults (shear zones) in the Earth's mantle. *Tectonophysics*, 558–559, 1–27. <https://doi.org/10.1016/j.tecto.2012.06.006>
- Vevers, J. J. (1994). Case for the Gamburtsev Subglacial Mountains of East Antarctic originating by mid-Carboniferous shortening of an intracratonic basement. *Geology*, 22, 593–596. [https://doi.org/10.1130/0091-7613\(1994\)022<0593:CFTGSM>2.3.CO;2](https://doi.org/10.1130/0091-7613(1994)022<0593:CFTGSM>2.3.CO;2)
- Wang, X., Ni, J., Aster, R., Sandvol, E., Wilson, D., Sine, C., et al. (2008). Shear wave splitting and mantle flow beneath the Colorado Plateau and its boundary with the Great Basin. *Bulletin of the Seismological Society of America*, 98, 2526–2532. <https://doi.org/10.1785/0120080107>
- Watson, T., Nyblade, A., Wiens, D. A., Anandakrishnan, S., Benoit, M., Shore, P. J., et al. (2006). P and S velocity structure of the upper mantle beneath the Transantarctic Mountains, East Antarctic craton, and Ross Sea from travel time tomography. *Geochemistry, Geophysics, Geosystems*, 7, Q07005. <https://doi.org/10.1029/2005GC001238>
- Weaver, S. D., Storey, B. C., Pankhurst, R. J., Mukasa, S. B., DiVenere, V. J., & Bradshaw, J. D. (1994). Antarctica–New Zealand rifting and Marie Byrd Land lithospheric magmatism linked to ridge subduction and mantle plume activity. *Geology*, 22(9), 811–814. [https://doi.org/10.1130/0091-7613\(1994\)022<0811:ANZRAM>2.3.CO;2](https://doi.org/10.1130/0091-7613(1994)022<0811:ANZRAM>2.3.CO;2)
- Wessel, P., Luis, J. F., Uieda, L., Scharroo, R., Wobbe, F., Smith, W. H. F., & Tian, D. (2019). The Generic Mapping Tools version 6. *Geochemistry, Geophysics, Geosystems*, 20, 5556–5564. <https://doi.org/10.1029/2019GC008515>
- White-Gaynor, A. L., & Nyblade, A. A. (2017). Shear wave splitting across the mid-Atlantic region of North America: A fossil anisotropy interpretation. *Geology*, 45(6), 555–558. <https://doi.org/10.1130/G38794.1>

- White-Gaynor, A. L., Nyblade, A. A., Aster, R. C., Wiens, D. A., Bromirski, P. D., Gerstoft, P., et al. (2019). Heterogeneous upper mantle structure beneath the Ross Sea Embayment and Marie Byrd Land, West Antarctica, revealed by P-wave tomography. *Earth and Planetary Science Letters*, 513, 40–50. <https://doi.org/10.1016/j.epsl.2019.02.013>
- Wiens, D. A., Shen, W., & Lloyd, A. (2021). The seismic structure of the Antarctic upper mantle. *Geological Society London Memoirs*, 56(17). <https://doi.org/10.1144/M56-2020-18>
- Wolfe, C. J., & Silver, P. G. (1998). Seismic anisotropy of oceanic upper mantle: Shear wave splitting methodologies and observations. *Journal of Geophysical Research: Solid Earth*, 103(B1), 749–771. <https://doi.org/10.1029/97JB02023>
- Wüstefeld, A., Bokelmann, G., Zaroli, C., & Barruol, G. (2008). SplitLab: A shear-wave splitting environment in MATLAB. *Computers & Geosciences*, 34, 515–528. <https://doi.org/10.1016/j.cageo.2007.08.002>
- Zhou, Z., Wiens, D. A., Shen, W., Aster, R. C., Nyblade, A. A., & Wilson, T. J. (2022). Radial Anisotropy and sediment thickness of West and Central Antarctica estimated from Rayleigh and Love wave velocities. *Journal of Geophysical Research: Solid Earth*, 127(3).